Research on Chemical Intermediates
https://doi.org/10.1007/s11164-021-04413-x

Transition metal (II) complexes of hydrazones derived from tetralone: synthesis, spectral characterization, in vitro antimicrobial and cytotoxic studies

J. Devi[1] · S. Sharma[1,2] · S. Kumar[1] · D. K. Jindal[3] · P. P. Dutta[4,6] · D. Kumar[5]

Received: 14 November 2020 / Accepted: 30 January 2021

Abstract

A series of transition metal (II) complexes with general formula $[M(L^{1-4})_2(H_2O)_2]$ (where M = Co(II), Ni(II), Cu(II) and Zn(II)) was synthesized by the reaction of metal(II) acetates with hydrazones $[HL^1–HL^4]$ obtained from condensation of tetralone with hydrazide derivatives. The characterization of synthesized compounds (1–20) was done by using elemental analysis, different spectral studies (UV–Vis, ^{1}H NMR, ^{13}C NMR, FT-IR, mass, ESR and fluorescence), magnetic susceptibility,

✉ J. Devi
jaya.gju@gmail.com

S. Sharma
somsamainia@gmail.com

S. Kumar
sanjeevbagri2221@gmail.com

D. K. Jindal
deepakjindal44@yahoo.com

P. P. Dutta
partha184@gmail.com

D. Kumar
guptadeepak002@gmail.com

[1] Department of Chemistry, Guru Jambheshwar University of Science and Technology, Hisar 125001, India

[2] Department of Chemistry, Government College Hisar, Hisar 125001, India

[3] Department of Pharmaceutical Sciences, Guru Jambheshwar University of Science and Technology, Hisar 125001, India

[4] Institute of Advanced Studies in Science & Technology, Life Science Division, Guwahati 781035, Assam, India

[5] School of Pharmaceutical Sciences, Shoolini University, Solan 173212, Himachal Pradesh, India

[6] Faculty of Pharmaceutical Science, Assam Down Town University, Panni khaiti, Guwahati 781026, Assam, India

Published online: 25 February 2021

molar conductance measurement and thermal (DTA, TGA and DTG) analysis. The characterization results suggested the bidentate nature of the hydrazones, which chelate with the metal ion via nitrogen of (C=N) group and deprotonated carbonyl oxygen in the enolized form, resulting in stable, non-volatile octahedral complexes. The antimicrobial potential of the compounds was evaluated against four bacterial, i.e. (*S. aureus*, *B. subtilis*, *P. aeruginosa and E. coli)*, and two fungal species, i.e. (*A. niger and C. albicans)*, by a serial dilution method with complexes 15 and 16 as most active compounds against microbes. All the compounds were also tested for its cytotoxicity (in vitro) against three human cancer cell lines (A549, HeLa and MCF-7) and one normal cell line (L_6) by the MTT assay, which focussed on an increased activity of compounds 7 and 15 towards A549, MCF-7 and HeLa cancer cell line with IC_{50} values ranging from 10.76 to 16.42 µg/mL, and compounds were found to be non-toxic towards L_6 cell line as compared to the standard drug doxorubicin. The results demonstrated that complexation enhanced the biological activity of compounds.

Graphic abstract

The synthesized compounds (1–20) were screened for antitumor activities against A549, MCF7, Hela cancer cell lines. Copper complex (7) and (15) was found to be the most active antitumor agent and less toxic against L6—Rat myoblast normal cell line than standard doxorubicin.

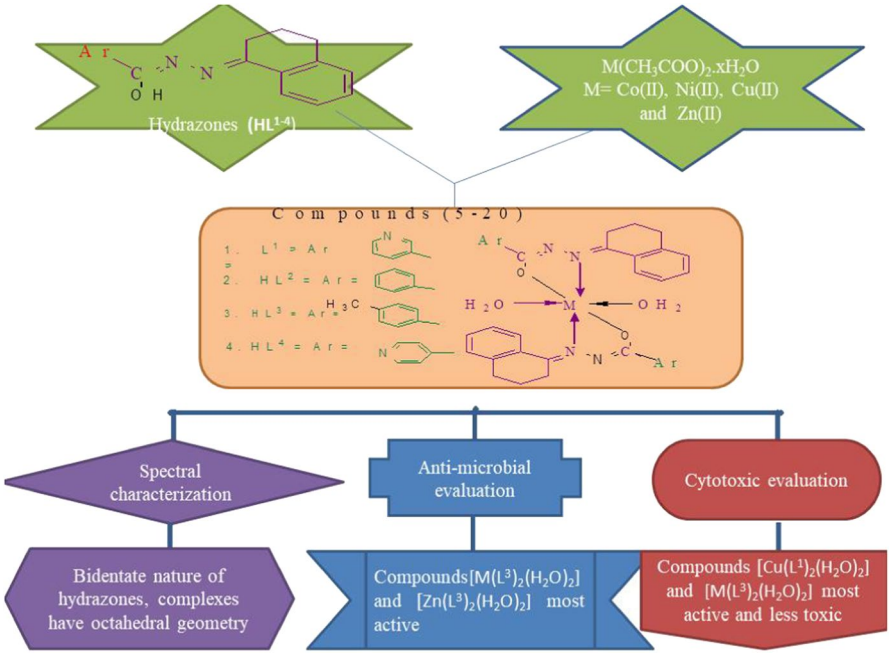

Keywords Hydrazone · Bidentate · Octahedral · Antimicrobial · Anticancer

Abbreviations

DME	M Dulbecco's modified Eagle's medium
DMF	Dimethylformamide
DMSO	Dimethyl sulfoxide
DMSO-d6	Deuterated dimethyl sulfoxide
ESR	Electron spin resonance
TGA	Thermal gravimetric analysis
DTA	Differential thermal analysis
MS	Mass spectra
FAB	Fast atom bombardment
FT-IR	Fourier transform infrared spectroscopy
A549	Human lung carcinoma cell line
HeLa	Human cervical carcinoma cell line
MCF7	Human breast carcinoma cell line
L_6	Rat myoblast cell line normal
MTT	3-(4,5-Dimethylthiazol-2-yl)-2,5- diphenyltetrazolium bromide
NMR	Nuclear magnetic resonance
IC_{50}	Concentration of drug required to inhibit the growth of 50% of tumour cells

Introduction

Cancer or malignant neoplasm is one of the most widespread and highly feared diseases for human life causing death nowadays in both developing and developed countries. Cancer results from the uncontrolled multiplication of ingenious modified normal human cells. Researchers throughout the globe have contributed significantly towards the anticancer drug development research. Cisplatin (*cis*-diamminedichloroplatinum(II)), a platinum metal-based drug, was a major development in cancer treatment [1], but its adverse effects such as sickness, kidney and liver failure, heavy metal toxicity and drug resistance [2] promoted researchers to discover new metallodrugs that are less toxic, economic, target specific with a higher efficiency.

In the last few decades, the applications of transition metal complexes for the medical therapy of cancer are extensively investigated, and consequently, they were acknowledged as promising anticancer agents. Transition metal complexes demonstrated various therapeutic properties and are widely used in medicine as well as have other applications also [3]. The ligand scaffolds play an important role in the chemotherapy, and among ligand system, hydrazones consisting of a carbon–nitrogen double bond (R–CO–NH–N=CHR) group [4] belong to special class due to their interesting multidentate chelating properties and form complexes with almost all the metal ions in different oxidation states depending upon the carbonyl group and hydrazide derivatives [5, 6]. They possess diverse biological and pharmaceutical activities [7, 8] such as antimicrobial [9, 10], anticancer [11, 12] and antioxidant properties [13]. They also show applications in wastewater treatment [14],

catalytical activity [15, 16], good magnetic behaviour [17], specific sensors, non-linear optical devices [18], resin for separation [19] and acting as enzyme inhibitor [20].

Tetralone, carbonyl entity is selected here for hydrazones' formation, represents an important compound in modern medicinal chemistry as it has considerable importance in biological field [21], anti-trypanosoma, antidepressant in sertraline drug, antimalarial [22], anticancer, antioxidant [23], anti-inflammatory agent [24] and as inhibitors of monoamine oxidase [25]. As a result to develop ingenious anti-cancer agent, huge number of transition metal complexes were synthesized from hydrazones and tested for anticancer activities, and many of them exhibited excellent activities [26]. The literature survey suggested that biological potential of compounds gets influenced by the coordination number of metal atom, structure of molecules and substituents attached to metal atom.

Due to the widespread therapeutic and diagnostic properties of hydrazones and tetralone derivatives, it seemed appealing to investigate compounds that have remarkable applications of both antimicrobial and anticancer activities, so here we have reported the synthesis of hydrazones from condensation of hydrazide derivatives with tetralone and reacted them with transition metal(II) acetates to form complexes. For characterization and structure determination, various spectroscopic analyses (UV–Vis, ^{1}H NMR, ^{13}C NMR, FT-IR, mass, ESR and fluorescence), magnetic susceptibility, elemental analysis, molar conductance measurements and thermal (TGA, DTG and DTA) methods were used. Screening of compounds for cytotoxic activity against three cancer cell lines—human breast adenocarcinoma cell line (MCF7), human alveolar adenocarcinoma epithelial cell line (A549), human cervical cell line (HeLa) and Rat myoblast cell line normal (L_6)—were assayed. The antimicrobial activity was also tested against four bacterial, i.e. (*S. aureus*, *B. subtilis*, *E. coli and P. aeruginosa)* and two fungal, i.e. (A. *niger, C. albicans)*, strains.

Experimental

Materials

The solvents, chemicals and reagents used for the research were of analytical grade. Hydrazide derivatives (nicotinic acid, benzoic acid, toluic acid and isonicotinic acid), α-tetralone and metal(II) acetates [$Co(CH_3COO)_2{\cdot}4H_2O$, $Ni(CH_3COO)_2{\cdot}4H_2O$, $Cu(CH_3COO)_2{\cdot}H_2O$ and $Zn(CH_3COO)_2{\cdot}2H_2O$] were purchased from Sigma-Aldrich company. The solvents used were dried as reported in the literature [27].

Instrumentation

Infrared spectra of hydrazones and their metal complexes were measured by using KBr pellets on Shimadzu IR affinity-I 8000 FT-IR spectrophotometer within the range of 400–4000 cm^{-1}. NMR spectra (^{1}H and ^{13}C) of hydrazones and their zinc(II) complexes were obtained in $CDCl_3$ by taking TMS as an internal reference

on Bruker Avance II 400 MHz NMR spectrometer. The coupling constant (J) and chemical shift (δ) were measured in Hz and ppm. Elemental (CHN) data were analysed by the instrument PerkinElmer 2400 elemental analyser. Standard gravimetric procedures were used to determine the metal percentage in the compounds, nickel as nickel dimethylglyoximate, zinc as zinc ammonium phosphate, cobalt as cobalt pyridine thiocyanate and copper as cupreous thiocyanate [28]. Electronic spectral data were obtained in DMSO by using UV–Vis–NIR Varian Cary-5000 spectrophotometer. ESR spectral analysis of the Cu(II) complexes was measured by taking tetracyanoethylene (TCNE) free radical as an internal reference on the Varian E112 X-band spectrometer. Gouy's procedure is used to calculate the magnetic susceptibilities of the compounds at 298 K by taking $Hg[Co(SCN)_4]$ as the reference to calibrate the instrument. Conductivity of 10^{-3} M solution was measured by using a model-306 Systronics conductivity bridge at 298 K in DMSO. The melting points (°C) of compounds were measured on a hot-stage Gallen Kamp melting point apparatus in open capillaries. Mass spectra of compounds were obtained by using API 2000 Applied Bio systems mass spectrometer in DMSO solvent. PerkinElmer Diamond TG/DTA thermogravimetric analyser is used to carry out thermal (TGA, DTG and DTA) study of compounds under nitrogen atmosphere with flow rate of 20 mL/min and heating rate 10 °C/min. Steady-state fluorescence spectra of hydrazones and their respective complexes were carried out on Shimadzu RF-5301 PC spectrophotometer.

Pharmacology

Antimicrobial assay

Hydrazones and their respective transition metal complexes were screened for their in vitro antimicrobial activity against four bacterial species: *Bacillus subtilis* (MTCC 8561), *Staphylococcus aureus* (MTCC 2901), *Pseudomonas aeruginosa* (MTCC 424), *Escherichia coli* (MTCC 16,521) and two fungal species: *Candida albicans* (MTCC 227), *Aspergillus niger* (MTCC 8189) by serial dilution method [29]. Test organisms were grown on nutrient agar (bacterial strain) and sabouraud dextrose (fungal strain) as nutrient medium. The stock solution was obtained by adding 2 mg of synthesized compounds in 10 mL DMSO. Further, to prepare a solution of 100 µg/mL concentration, 1 mL of this stock solution was poured into each test tube having 1 mL of nutrient broth/sabouraud dextrose broth. The solutions of 50, 25, 12.50 and 6.25 µg/mL concentrations were prepared by the serial dilution method. Microbial species were grown at 37 °C for 24 h in case of the bacterial and at 25 °C for one week in case of the fungal strains. Ciprofloxacin is used as a reference drug for antibacterial and fluconazole for antifungal activity, and their activity was also performed by taking DMSO as negative control. After incubation, the data were observed at various concentrations and calculated their MIC values in µ mol/mL. The microbial activity of compounds was carried out in duplicate to minimize error, and an average value is reported here.

Cytotoxic assay

The in vitro anticancer activity of the compounds (1–20) was tested as given by Mosmann [30]. The cytotoxicity was evaluated against a series of three different human carcinoma cell lines: A549 derived from human alveolar adenocarcinoma epithelial cell lines (ATCC No.CCL-185), HeLa derived from human cervical adenocarcinoma epithelial cell lines (ATCC No. CCL-2), MCF7 derived from human breast adenocarcinoma epithelial cell lines (ATCC No.HTB-22) as well as normal cell line L_6 derived from rat skeletal muscle myoblast cells (ATCC No. CRL-1458), and these cells were cultured in Dulbecco's modified Eagle's medium (DMEM) supplemented with 1% gentamicin, 10% foetal bovine serum (FBS) and 10% Pen-Strep. Briefly, cells (1×10^6 per mL) were seeded in tissue culture grade multiwall plates in complete medium and incubated under standard conditions in 37 °C humidified 5% CO_2 atmosphere. The complete medium was replaced after one day with FBS-free medium and incubated overnight. The cells were then treated with the samples in various concentrations into each well and incubated for 24 h. Well containing medium alone (untreated cells) was served as a control. After the incubation period, 10 µL of MTT (5 mg/mL) was poured to each well, mixed thoroughly and incubated again for 4 h. After the incubation period, cells were seen with the help of inverted microscope for the existence of dark purple crystals of formazan at the bottom of the wells. Isopropanol (100 µL) with 0.04 M HCl was poured to each well and mixed it completely by repeated pipetting with a multi-channel pipette. The HCl converts the phenol red in tissue culture medium to a yellow colour that does not interfere with the MTT formazan measurement. The isopropanol dissolves the formazan to give a homogeneous blue solution suitable for absorbance calculation, and absorbance was calculated by ELISA plate reader (Filter Max F_3 Multi-Mode Micro plate Readers, Molecular Devices) with a test wavelength of 570 nm and a reference wavelength of 630 nm. The effect of the samples on the proliferation of cells was expressed as the % inhibition of cell proliferation and measured as (Absorbance of control cells—Absorbance of treated cells/Absorbance of control cells) × 100. Cytotoxic concentration (IC_{50}) of the samples was calculated by the dose–response curves. The anticancer data are mean ± standard deviation and were taken as the average of three sets of readings of independent trials by taking doxorubicin as reference drug.

Synthesis

Synthesis of hydrazones (HL^1–HL^4) (1–4)

The hydrazones: nicotinic acid (3,4-dihydro-2H-naphthalen-1-ylidene)-hydrazide HL^1/benzoic acid (3,4-dihydro-2H-naphthalen-1-ylidene)-hydrazide HL^2/4-methyl-benzoic acid (3,4-dihydro-2H-naphthalen-1-ylidene)-hydrazide HL^3/isonicotinic acid (3,4-dihydro-2H-naphthalen-1-ylidene)-hydrazide HL^4 were synthesized by the condensation of tetralone (0.438 g, 3.0 mmol) with nicotinic (0.411 g) HL^1/benzoic (0.408 g) HL^2/p-toluic (0.450 g) HL^3/isonicotinic (0.411 g) HL^4 acid hydrazide (3.0 mmol) under refluxing in ethanol (20 mL) for

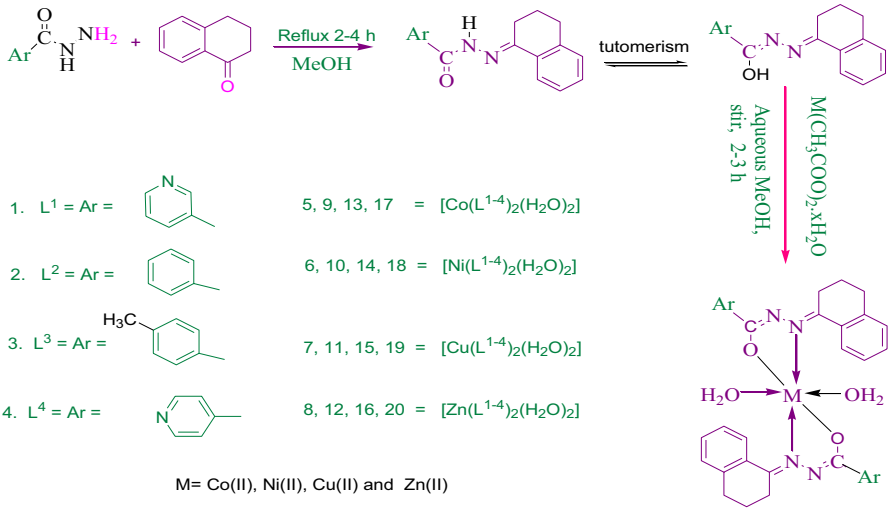

Scheme 1 Synthesis of hydrazones (1–4) and their transition metal complexes (5–20)

2–4 h in equimolar ratio under constant stirring. The reaction progress was regularly monitored by TLC. The light colour solid compounds were separated by filtration, washed with methanol, dried under vacuum over anhydrous calcium chloride, and recrystallized from chloroform to obtain pure hydrazones (Scheme 1).

Nicotinic acid (3,4-dihydro-2H-naphthalen-1-ylidene)-hydrazide (HL^1)

Yield: 87%; Colour: Light yellow; M.p.: 75–78 °C; Conductivity: ($ohm^{-1}cm^2\ mol^{-1}$) in DMSO: 12; $C_{16}H_{15}N_3O$: Anal. Cald: C, 72.43; H, 5.70; N, 15.84, Found: C, 72.42; H, 5.73; N, 15.87; MS: *m/z* (M^+) Cald: 265.31; Found:266.7077 $(M+1)^+$; FT-IR (KBr, ν, cm^{-1}): 1653 ν(C=O, carbonyl), 3258 ν(–NH),1615 ν(–C=N), 1013 ν(–N–N–H); ^{1}H NMR [400 MHz, $CDCl_3$, δ(ppm)]: 9.26 (*s*, *t*, 1H, N=C–OH), 7.85 (*d*, $J=4$ Hz, 1H, C_5'–H), 7.51 (*d*, $J=8$ Hz, 1H, C_9–H), 7.21 (*d*, $J=8$ Hz, 2H, C_6–H), 7.18 (*d*, $J=8$ Hz, 2H, C_7–H), 8.78 (*s*, 1H, C_2'–H), 7.36 (*t*, $J=8$ Hz, 1H, C_8–H), 7.25 (*t*, $J=4$ Hz, 1H, C_4'–H), 8.30 (*s*, 2H, C_3'–H), 2.85 (*t*, $J=6$ Hz, 2H, C_4–H), 2.71 (*t*, $J=6$ Hz, 2H, C_2–H), 2.04 (*m*, $J=6$ Hz, 2H, C_3–H);^{13}C NMR:[100 MHz, $CDCl_3$, δ(ppm)]: 166.38 (HNC=O), 151.70 (C_1), 139.66 (C_2'), 131.95 (C_5'), 129.94 (C_9), 137.92 (C_5), 122.92 (C_4'), 133.90 (C_3'), 133.60 (C_1'), 128.93 (C_8), 126.61 (C_6), 124.21 (C_7), 120.12 (C_{10}), 29.93 (C_4), 24.58 (C_2), 21.27 (C_3).

Benzoic acid (3,4-dihydro-2H-naphthalen-1-ylidene)-hydrazide (HL^2)

Yield: 82%; Colour: white; M.p.: 72–75 °C; Conductivity: ($ohm^{-1}cm^2mol^{-1}$) in DMSO: 11, $C_{17}H_{16}N_2O$: Anal. Cald: C, 77.25; H, 6.10; N, 10.60, Found.: C, 77.22; H, 6.08; N, 10.58, MS: m/z (M^+) Cald: 264.12; Found:265.1241 $(M+1)^+$; FT-IR (KBr, ν, cm^{-1}): 1648 ν(C=O, carbonyl), 3242 ν(–NH),1612 ν(–C=N), 1013 ν(–N–N–H); ^{1}H NMR [400 MHz, $CDCl_3$, δ(ppm)]: 9.01 (*s*, ^{1}H, N=C–OH), 8.38 (*s*, 1H, C_9–H), 7.89 (*d*, 2H, $J=12$ Hz, C_2'–H and C_6'–H), 7.59 (*t*, $J=12$ Hz, 1H, C_4'–H), 7.52 (*t*, $J=12$ Hz, 2H, C_3'–H and C_5'–H), 7.28 (*d*, 1H, C_8–H. $J=8$ Hz), 7.16 (*d*, $J=8$ Hz,2H, C_6–H and C_7–H), 2.85 (*t*, $J=6$ Hz, 2H, C_4–H), 2.68 (*t*, $J=6$ Hz, 2H, C_2–H), 2.03 (*m*, $J=6$ Hz, 2H, C_3–H); ^{13}C NMR:[100 MHz, $CDCl_3$, δ(ppm)]: 161.31 (HNC=O), 150.62 (C_1), 139.63 (C_5), 135.93 (C_1'), 128.12 (C_9), 131.27 (C_2'), 129.17 (C_6'), 133.61 (C_4'), 130.59 (C_3'), 127.88 (C_5'), 126.61 (C_8), 125.55 (C_6), 125.25 (C_7), 121.18 (C_{10}), 29.62 (C_4), 25.25 (C_2), 21.61 (C_3).

4-Methyl-benzoic acid (3,4-dihydro-2H-naphthalen-1-ylidene)-hydrazide (HL^3)

Yield: 79%; Colour: white; M.p.: 74–76 °C; Conductivity: ($ohm^{-1}cm^2$ mol^{-1}) in DMSO: 12; $C_{18}H_{18}N_2O$: Anal. Cald: C, 77.67; H, 6.52; N, 10.06, Found.: C, 77.65; H, 6.50; N, 10.05, MS: m/z (M^+) Cald: 278.15; Found:279.1575 $(M+1)^+$; FT-IR (KBr, ν, cm^{-1}): 1645 ν(C=O, carbonyl), 3246 ν(–NH),1610 ν(–C=N), 1015 ν(–N–N–H); ^{1}H NMR [400 MHz, $CDCl_3$, δ(ppm)]: 9.04 (*s*, ^{1}H, N=C–OH), 8.37 (*s*, 1H, C_9–H), 7.31 (*d*, $J=8.4$ Hz, 2H, C_2'–H and C_6'–H), 7.28 (*d*, $J=8.4$ Hz, 2H, C_3'–H and C_5'–H), 7.81 (*t*, $J=8$ Hz, 1H, C_8–H), 7.16 (*d*, $J=8$ Hz, 2H, C_6–H and C_7–H), 2.85 (*t*, $J=6.0$ Hz, 2H, C_4–H), 2.67 (*t*, $J=6$ Hz, 2H, C_2–H), 2.04 (*m*, $J=6$ Hz, 2H, C_3–H), 2.45 (*s*, 3H, $-CH_3$); ^{13}C NMR: [100 MHz, $CDCl_3$, δ(ppm)]: 163.63 (HNC=O), 153.64 (C_1), 139.92 (C_5), 132.54 (C_1'), 130.20, (C_9), 127.90 (C_2'), 126.23 (C_6'), 133.58 (C_4'), 128.56 (C_3'), 127.58 (C_5'), 126.91 (C_8), 124.57 (C_6), 123.88 (C_7), 122.24 (C_{10}), 29.62 (C_4), 23.29 (-CH_3), 25.17 (C_2), 21.58 (C_3).

Isonicotinic acid (3,4-dihydro-2H-naphthalen-1-ylidene)-hydrazide (HL^4)

Yield: 78%; Colour: white; M.p.: 77–79 °C; Conductivity: (ohm^{-1} cm^2 mol^{-1}) in DMSO: 13.; $C_{16}H_{15}N_3O$: Anal. Cald: C, 72.43; H, 5.71; N, 15.85, Found.: C, 72.42; H, 5.73; N, 15.87; MS: m/z (M^+) Cald: 265.12; Found: 266.1277 $(M+1)^+$; FT-IR (KBr, ν, cm^{-1}): 1655 ν(C=O, carbonyl), 3248 ν(–NH),1611 ν(–C=N), 1018 ν(–N–N–H); ^{1}H NMR [400 MHz, $CDCl_3$, δ(ppm)]: 9.86 (*s*, ^{1}H, N=C–OH), 8.24 (*s*, 1H, C_9–H), 7.66 (*d*, $J=8$ Hz, 2H, C_2'–H and C_5'–H), 8.67 (*d*, $J=8$ Hz, 2H, C_3'–H and C_4'–H), 7.06 (*t*, $J=6.2$ Hz, 1H, C_8–H), 7.16 (*d*, $J=6.2$ Hz, 2H, C_6–H and C_7–H), 2.85 (*t*, $J=6$ Hz, 2H, C_4–H), 2.71 (*t*, $J=6$, Hz, 2H, C_2–H), 2.04 (*m*, $J=6$ Hz, 2H, C_3–H); ^{13}C NMR:[100 MHz, $CDCl_3$, δ(ppm)]: 162.37 (HNC=O), 147.15 (C_1), 142.99 (C_5), 133.22(C_1'), 126.85(C_9), 128.55 (C_2'), 131.26 (C_3'), 130.22 (C_4'), 128.23 (C_5'), 129.24 (C_8), 127.20 (C_6), 123.90 (C_7), 121.17 (C_{10}), 29.61 (C_4), 26.79(C_2), 21.58 (C_3).

Synthesis of transition metal complexes $[M(L^{1-4})_2(H_2O)_2]$ (5–20)

To the methanolic solution (20 mL) of metal acetates $[M(CH_3COO)_2{\cdot}xH_2O]$ of cobalt (0.248 g, 1.0 mmol)/nickel (0.248 g, 1.0 mmol)/copper (0.198 g, 1.0 mmol)/zinc (0.220 g, 1.0 mmol) was added a hot aqeuous methanolic solution (20 mL) of hydrazones HL^1 (0.530 g, 2.0 mmol)/HL^2(0.528 g, 2.0 mmol)/HL^3 (0.556 g, 2.0 mmol)/HL^4 (0.530 g, 2.0 mmol) with constant stirring in 1:2 molar ratio for 2–3 h. To maintain the pH of the solution, NaOH was added to it. The separated compounds were filtered, recrystallized with methanol and washed with hexane to separate out unreacted metal acetates to obtain pure product (Scheme 1).

$Co(L^1)_2(H_2O)_2]$

Yield: 73%; Colour: Reddish brown; M.p.: 180–85 °C; Conductivity: (ohm^{-1} cm^2 mol^{-1}) in DMSO: 17; $C_{32}H_{32}CoN_6O_4$; Anal. Cald: C, 61.63; H, 5.18; N, 13.45, Co, 9.46;Found.: C, 61.64; H, 5.17; N, 13.48; MS: m/z (M^+) Cald: 623.5982; Found:624.5712 $(M+1)^+$; FT-IR (KBr, ν, cm^{-1}): 1253 ν(C–O), 3427 ν(coordinated water),1598 ν(–C=N), 1018 ν(–N–N–H), 545 ν(Co–O), 435 ν(Co–N).

$[Ni(L^1)_2(H_2O)_2]$

Yield: 75%; Colour: Green; M.p.: 197–99 °C; Conductivity: (ohm^{-1} cm^2 mol^{-1}) in DMSO: 12; $C_{32}H_{32}NiN_6O_4$; Anal. Cald: C, 61.69; H, 5.48; N, 13.43, Ni, 9.40; Found.: C, 61.66; H, 5.17; N, 13.48; MS: m/z (M^+) Cald: 623.3573; Found: 624.3307 $(M+1)^+$; FT-IR (KBr, ν, cm^{-1}): 1245 ν(C-O), 3425 ν(coordinated water),1594 ν(–C=N), 1021 ν(–N–N–H), 547 ν(Ni–O), 440 ν(Ni–N).

$[Cu(L^1)_2(H_2O)_2]$

Yield: 78%; Colour: Brown; M.p.: 194–97 °C; Conductivity: (ohm^{-1} cm^2 mol^{-1}) in DMSO: 18; $C_{32}H_{32}CuN_6O_4$; Anal. Cald: C, 61.19; H, 5.13; N, 13.35, Cu, 10.09; Found.: C, 61.18; H, 5.13; N, 13.38, MS: m/z (M^+) Cald: 628.2035; Found:629.1889 $(M+1)^+$; FT-IR (KBr, ν, cm^{-1}): 1248 ν(C-O), 3428 ν(coordinated water),1595 ν(–C=N), 1023 ν(–N–N–H), 543 ν(Cu–O), 442 ν(Cu–N).

$[Zn(L^1)_2(H_2O)_2]$

Yield: 76%; Colour: Reddish brown; M.p.: 192–95 °C; Conductivity: (ohm^{-1} cm^2 mol^{-1}) in DMSO: 19; $C_{32}H_{32}ZnN_6O_4$; Anal. Cald: C, 61.02; H, 5.11; N, 13.31, Zn:10.38; Found.: C, 61.00; H, 5.12; N, 13.34; MS: m/z (M^+) Cald: 630.0549; Found: 631.0265 $(M+1)^+$; FT-IR (KBr, ν, cm^{-1}): 1233 ν(C–O), 3430 ν(coordinated water),1586 ν(–C=N), 1029 ν(–N–N–H), 548 ν(Zn–O), 439 ν(Zn–N), ^{1}H NMR [400 MHz, $CDCl_3$, δ(ppm)]: 7.85 (*d*, $J=4$ Hz, 1H, C_5'–H), 7.51 (*d*,

$J=8$ Hz, 1H, C_9–H), 8.52 (*d*, $J=8$ Hz, 1H, C_2'–H), 7.25 (*t*, $J=4$ Hz, 1H, C_4'–H), 8.07 (*s*, 2H, C_3'–H); 7.35 (*t*, $J=8$ Hz, 1H, C_8–H), 7.21 (*d*, $J=8$ Hz, 2H, C_6–H), 7.18 (*d*, $J=8$ Hz, 2H, C_7–H), 2.86 (*t*, $J=6.2$ H, 2H, C_4–H), 2.70 (*t*, $J=5.2$ Hz, 2H, C_2-H), 2.44 (*s*, 2H, H_2O), 2.04 (*m*, $J=6.8$ Hz, 2H, C_3-H); ^{13}C NMR:[100 MHz, $CDCl_3$, δ(ppm)]: 169.02 (N=C–OH), 152.79 (C_1), 139.60 (C_2'), 131.93 (C_5'), 129.84 (C_9), 137.94 (C_5), 122.92 (C_4'), 133.91 (C_3'), 133.62 (C_1'), 128.97 (C_8), 126.62 (C_6), 124.22 (C_7), 120.16 (C_{10}), 29.96 (C_4), 24.23 (C_2), 21.35(C_3).

$[Co(L^2)_2(H_2O)_2]$

Yield: 77%; Colour: Reddish brown; M.p.: 195–97 °C; Conductivity: (ohm^{-1} cm^2 mol^{-1}) in DMSO: 16; $C_{34}H_{34}CoN_4O_4$; Anal. Cald: C, 65.72; H, 5.51; N, 9.04; Co, 9.45; Found.: C, 65.70; H, 5.51; N, 5.01, MS: m/z (M^+) Cald: 621.3527; Found:622.6552 $(M+1)^+$; FT-IR (KBr, ν, cm^{-1}): 1249 ν(C–O), 3417 ν(coordinated water),1591 ν(–C=N), 1016 ν(–N–N–H), 540 ν(Co–O), 426 ν(Co–N).

$[Ni(L^2)_2(H_2O)_2]$

Yield: 79%; Colour: Green; M.p.: 227–32 °C; Conductivity: (ohm^{-1} cm^2 mol^{-1}) in DMSO: 14; $C_{34}H_{34}NiN_4O_4$; Anal. Cald: C, 65.71; H, 5.51; N, 9.04; Ni, 9.43; Found.: C, 65.72; H, 5.52; N, 9.02; MS: m/z (M^+) Cald: 621.5978; Found: 622.6252 $(M+1)^+$; FT-IR (KBr, ν, cm^{-1}): 1267, ν(C-O), 3415 ν(coordinated water),1588 ν(–C=N), 1017 ν(–N–N–H), 542 ν(Ni–O), 422 ν(Ni–N).

$[Cu(L^2)_2(H_2O)_2]$

Yield: 72%; Colour: Brown; M.p.: 216–19 °C; Conductivity: ($ohm^{-1}cm^2$ mol^{-1}) in DMSO: 17; $C_{34}H_{34}CuN_4O_4$; Anal. Cald: C, 65.23; H, 5.48; N, 8.92,Cu, 10.12; Found.: C, 65.21; H, 5.47; N, 8.92; MS: m/z (M^+) Cald: 627.2047; Found:628.2396 $(M+1)^+$; FT-IR (KBr, ν, cm^{-1}): 1248 ν(C–O), 3422 ν(coordinated water),1589 ν(–C=N), 1018 ν(–N–N–H), 539 ν(Cu–O), 425 ν(Cu–N).

$[Zn(L^2)_2(H_2O)_2]$

Yield: 75%; Colour: Reddish brown; M.p.: 218–22 °C; Conductivity: (ohm^{-1} cm^2 mol^{-1}) in DMSO: 20; $C_{34}H_{34}ZnN_6O_4$; Anal. Cald: C, 65.04; H, 5.45; N, 8.92, Zn; 10.38; Found.: C,65.02; H,5.46; N, 8.91; MS: m/z (M^+) Cald: 628.0767; Found:629.0546 $(M+1)^+$; FT–IR (KBr, ν, cm^{-1}): 1253 ν(C–O), 3425, ν(coordinated water),1585 ν(–C=N), 1019 ν(–N–N–H), 537 ν(Zn–O), 427 ν(Zn–N); ^{1}H NMR [400 MHz, $CDCl_3$, δ(ppm)]: 8.32 (d, 1H, C_9–H), 7.88 (*d*, $J=12$, Hz 2H, C_2'–H and C_6'–H), 7.61 (*t*, $J=12$ Hz, 1H, C_4'–H), 7.52 (*t*, $J=12$ Hz, 2H, C_3'–H and C_5'–H), 7.28 (*d*, $J=8$ Hz, 1H, C_8–H), 7.16 (*d*, $J=8$ Hz, 2H, C_6–H and C_7–H), 2.84 (*t*, $J=6$ Hz, 2H, C_4–H), 2.68 (*t*, $J=6$ Hz, 2H, C_2–H), 2.03 (*m*, $J=6$ Hz, 2H, C_3–H),

2.40 (*s*, 2H, H_2O); ^{13}C NMR:[100 MHz, $CDCl_3$, δ(ppm)]: 164.02 (N=C–OH), 153.63(C_1), 142.26 (C_5), 135.95(C_1'), 128.54 (C_9), 131.94 (C_2'), 129.91 (C_6'), 133.23 (C_4'), 130.60 (C_3'), 127.58 (C_4'), 126.61 (C_8), 125.55 (C_6), 125.25 (C_7), 121.19 (C_{10}), 29.63 (C_4), 25.23 (C_2), 20.28 (C_3).

$[Co(L^3)_2(H_2O)_2]$

Yield: 73%; Colour: Reddish brown; M.p.: 178–181 °C; Conductivity: ($ohm^{-1}cm^2\ mol^{-1}$) in DMSO: 13; $C_{36}H_{38}CoN_4O_4$; Anal. Cald: C: 66.55; H: 5.92; N, 8.65, Co, 9.04; Found.: C, 66.56; H, 5.90; N, 8.62; MS: m/z (M^+) Cald: 649.6586; Found:650.2863 $(M+1)^+$; FT-IR (KBr, ν, cm^{-1}): 1262, ν(C–O), 3431 ν(coordinated water),1599 ν(–C=N), 1021 ν(–N–N–H), 547 ν(Co–O), 434, ν(Co–N).

$[Ni(L^3)_2(H_2O)_2]$

Yield: 75%; Colour: Green; M.p.: 214–218 °C; Conductivity: ($ohm^{-1}\ cm^2\ mol^{-1}$) in DMSO: 16; $C_{36}H_{38}NiN_4O_4$; Anal. Cald: C, 66.57; H, 5.91; N, 8.60,,Ni, 9.01; Found.: C, 66.58; H, 5.90; N, 8.63; MS: m/z (M^+) Cald: 649.4219.; Found:650.4258 $(M+1)^+$; FT-IR (KBr, ν, cm^{-1}): 1225 ν(C–O), 3434, ν(coordinated water),1590 ν(–C=N), 1023 ν(–N–N–H), 540 ν(Ni–O), 435 ν(Ni–N).

$[Cu(L^3)_2(H_2O)_2]$

Yield: 78%; Colour: Brown; M.p.: 192–96 °C; Conductivity: ($ohm^{-1}cm^2\ mol^{-1}$) in DMSO: 17; $C_{36}H_{38}CoN_6O_4$; Anal. Cald: C, 66.07; H, 5.84; N, 8.56;Cu, 9.69; Found.: C, 66.09; H, 5.85; N, 8.51; MS: m/z (M^+) Cald: 654.3189; Found:655.4115 $(M+1)^+$; FT-IR (KBr, ν, cm^{-1}): 1234 ν(C–O), 3437 ν(coordinated water),1591 ν(–C=N), 1025 ν(–N–N–H), 554 ν(Cu–O), 437 ν(Cu–N).

$[Zn(L^3)_2(H_2O)_2]$

Yield: 76%; Colour: white; M.p.: 193–93 °C; Conductivity: ($ohm^{-1}\ cm^2\ mol^{-1}$) in DMSO: 18; $C_{36}H_{38}CoN_6O_4$; Anal. Cald: C, 65.92; H, 5.83; N, 8.51, Zn:9.71; Found: C, 65.90; H, 5.84; N, 8.54; MS: m/z (M^+) Cald: 656.1274; Found:657.1084 $(M+1)^+$; FT-IR (KBr, ν, cm^{-1}): 1255 ν(C–O), 3435 ν(coordinated water),1592 ν(–C=N), 1024 ν(–N–N–H), 550 ν(Zn–O), 431 ν(Zn–N); ^1H NMR [400 MHz, $CDCl_3$, δ(ppm)]:. 8.21(*d*, $J=8$ Hz, 1H, C_9–H), 7.30 (*t*, $J=8.4$ Hz, 1H, C_4'–H and C_2'–H), 7.28 (*d*, $J=8.4$ Hz, 2H, C_3'–H and C_5'–H), 7.62 (*t*, $J=8$ Hz, 1H, C_8–H), 7.16 (*d*, $J=8$ Hz, 2H, C_6–H and C_7–H), 2.85 (*t*, $J=6$ Hz, 2H, C_4–H), 2.67 (*t*, $J=6$ Hz, 2H, C_2–H), 2.03 (*m*, $J=6$ Hz, 2H, C_3–H), 2.46 (*s*, 3H, $–CH_3$), 2.38 (*s*, 2H, H_2O); ^{13}C NMR:[100 MHz, $CDCl_3$, δ(ppm)]: 165.37 (N=C–OH), 154.62 (C_1), 143.61 (C_5), 132.54 (C_1'), 130.20, (C_9), 127.90 (C_2'), 126.23 (C_6'), 133.58 (C_4'), 128.56 (C_3'), 129.74 (C_4'), 127.98 (C_5'), 126.91 (C_8), 124.44 (C_6), 123.86 (C_7), 122.25 (C_{10}), 29.62 (C_4), 23.19 ($–CH_3$), 25.27 (C_2), 21.58 (C_3).

$[Co(L^4)_2(H_2O)_2]$

Yield: 75%; Colour: Reddish brown; M.p.: 213–16 °C; Conductivity: ($ohm^{-1}cm^2\ mol^{-1}$) in DMSO: 15; $C_{32}H_{32}CoN_6O_4$; Anal. Cald: C, 61.61; H, 5.15; N, 13.49, Co, 9.43; Found.: C, 61.64; H, 5.17; N, 13.48; MS: m/z (M^+) Cald: 625.1068; Found:626.1076 $(M+1)^+$; FT-IR (KBr, ν, cm^{-1}): 1253 ν(C–O), 3437 ν(coordinated water),1588 ν(–C=N), 1018 ν(–N–N–H), 545 ν(Co–O), 442 ν(Co–N).

$[Ni(L^4)_2(H_2O)_2]$

Yield: 74%; Colour: Green; M.p.: 242–46 °C; Conductivity: ($ohm^{-1}cm^2mol^{-1}$) in DMSO: 17; $C_{32}H_{32}NiN_6O_4$; Anal. Cald: C, 61.67; H, 5.20; N, 13.49, Ni, 9.44; Found.: C, 61.66; H, 5.17; N, 13.48; MS: m/z (M^+) Cald: 625.1768; Found:626.3393 $(M+1)^+$; FT-IR (KBr, ν, cm^{-1}): 1232 ν(C–O), 3440 ν(coordinated water),1584 ν(–C=N), 1021 ν(–N–N–H), 546 ν(Ni–O), 436 ν(Ni–N).

$[Cu(L^4)_2(H_2O)_2]$

Yield: 77%; Colour: Brown; M.p.: 223–28 °C; Conductivity: ($ohm^{-1}cm^2\ mol^{-1}$) in DMSO: 18; $C_{32}H_{32}CoN_6O_4$; Anal. Cald: C, 61.20; H, 5.15; N, 13.37,Cu, 10.14; Found.: C, 61.18; H, 5.13; N, 13.38; MS: m/z (M^+) Cald: 628.1557; Found:629.4533 $(M+1)^+$; FT-IR (KBr, ν, cm^{-1}): 1228 ν(C–O), 3448 ν(coordinated water),1593 ν(–C=N), 1023 ν(–N–N–H), 543 ν(Cu–O), 440 ν(Cu–N).

$[Zn(L^4)_2(H_2O)_2]$

Yield: 79%; Colour: white; M.p.: 230–33 °C; Conductivity: ($ohm^{-1}\ cm^2\ mol^{-1}$) in DMSO: 19; $C_{32}H_{34}CoN_6O_4$; Anal. Cald: C, 61.03; H, 5.14; N, 13.33, Zn: 10.40; Found.: C, 61.00; H, 5.12; N, 13.34; MS: m/z (M^+) Cald: 630.0523; Found:631.1550 $(M+1)^+$; FT-IR (KBr, ν, cm^{-1}): 1253 ν(C–O), 3446 ν(coordinated water),1596 ν(–C=N), 1029 ν(–N–N–H), 547 ν(Zn–O), 445 ν(Zn–N); ^{1}H NMR [400 MHz, $CDCl_3$, δ(ppm)]: 8.03 (*s*, 1H, C_9–H), 7.66 (*d*, $J=8$ Hz, 2H, C_2'–H and C_5'–H), 8.66 (*d*, $J=8$ Hz, 2H, C_3'–H and C_4'–H), 7.06 (*t*, $J=6.2$ Hz, 1H, C_8–H), 7.16 (*d*, $J=6.2$ Hz, 2H, C_6–H and C_7–H), 2.85 (*t*, $J=6$ Hz, 2H, C_4–H), 2.68 (*t*, $J=6$ Hz, 2H, C_2–H), 2.04 (*m*, $J=6$ Hz, 2H, C_3–H), 2.40 (*s*, 2H, H_2O); ^{13}C NMR:[100 MHz, $CDCl_3$, δ(ppm)]: 166.34 (N=C–OH), 149.63 (C_1), 142.95(C_5), 133.22(C_1'), 126.85(C_9), 128.55 (C_2'), 131.26 (C_3'), 130.22 (C_4'), 128.23 (C_5'), 129.24 (C_8), 127.20 (C_6), 123.90 (C_7), 121.17 (C_{10}), 29.61 (C_4), 26.31(C_2), 21.28 (C_3).

Results and discussion

The hydrazones were synthesized by the condensation of respective hydrazide derivative with tetralone in equimolar ratio under refluxing in ethanol, and their transition metal complexes were obtained by reacting with Co(II), Ni(II), Cu(II) and Zn(II)

Table 1 Analytical and physical data of the synthesized compounds

C. no.	Compounds	Molecular formula	Colour	Molecular weight (Cal., M^+) *m/z* (found, $M+1^+$)	Yield (%)	Elemental analysis (%) Cal. (found)				Λ_m	M.P (°C)
						C	H	N	M		
1	HL^1	$C_{16}H_{15}N_3O$	Light yellow	265.31 (266.70)	87	72.43 (72.42)	5.70 (5.73)	15.84 (15.87)	–	12	76
2	HL^2	$C_{17}H_{16}N_2O$	white	264.12 (265.12)	82	77.25 (77.22)	6.10 (6.08)	10.60 (10.58)	–	13	73
3	HL^3	$C_{18}H_{18}N_2O$	white	278.15 (279.15)	79	77.67 (77.65)	6.52 (6.50)	10.06 (10.05)	–	11	75
4	HL^4	$C_{16}H_{15}N_3O$	white	265.12 (266.16)	80	72.43 (72.42)	5.71 (5.73)	15.85 (15.87)	–	13	78
5	$[Co(L^1)_2(H_2O)_2]$	$C_{32}H_{32}CoN_6O_4$	Reddish-brown	623.59 (624.57)	73	61.63 (61.64)	5.18 (5.17)	13.45 (13.48)	9.46 (9.45)	17	183
6	$[Ni(L^1)_2(H_2O)_2]$	$C_{32}H_{32}NiN_6O_4$	Green	623.35 (624.33)	75	61.69 (61.66)	5.18 (5.17)	13.46 (13.48)	9.40 (9.42)	15	198
7	$[Cu(L^1)_2{\cdot}(H_2O)_2]$	$C_{32}H_{32}CuN_6O_4$	Brown	628.20 (629.18)	78	61.19 (61.18)	5.13 (5.13)	13.35 (13.38)	10.09 (10.12)	18	195
8	$[Zn(L^1)_2(H_2O)_2]$	$C_{32}H_{32}ZnN_6O_4$	White	630.05 (631.02)	76	61.02 (61.00)	5.11 (5.12)	13.31 (13.34)	10.37 (10.38)	19	193
9	$[Co(L^2)_2(H_2O)_2]$	$C_{34}H_{34}CoN_4O_4$	Reddish brown	621.59 (622.62)	77	65.72 (65.70)	5.50 (5.51)	5.03 (5.01)	9.45 (9.48)	16	196
10	$[Ni(L^2)_2(H_2O)_2]$	$C_{34}H_{34}NiN_4O_4$	Green	621.35 (622.32)	79	65.71 (65.72)	5.51 (5.52)	9.04 (9.02)	9.43 (9.45)	14	228
11	$[Cu(L^2)_2{\cdot}(H_2O)_2]$	$C_{34}H_{34}CuN_4O_4$	Brown	626.20 (627.23)	72	65.23 (65.21)	5.48 (5.47)	8.92 (8.95)	10.12 (10.15)	17	218
12	$[Zn(L^2)_2(H_2O)_2]$	$C_{34}H_{34}ZnN_4O_4$	White	628.07 (629.05)	75	65.04 (65.02)	5.45 (5.46)	8.92 (8.91)	10.38 (10.41)	20	219
13	$[Co(L^3)_2(H_2O)_2]$	$C_{36}H_{38}CoN_4O_4$	Reddish-brown	649.65 (650.20)	73	66.55 (66.56)	5.92 (5.90)	8.65 (8.62)	9.04 (9.07)	13	179
14	$[Ni(L^3)_2(H_2O)_2]$	$C_{36}H_{38}NiN_4O_4$	Green	649.42 (650.42)	75	66.57 (66.58)	5.91 (5.90)	8.60 (8.53)	9.01 (9.04)	16	217
15	$[Cu(L^3)_2{\cdot}(H_2O)_2]$	$C_{36}H_{38}CuN_4O_4$	Brown	654.31 (655.41)	78	66.07 (66.09)	5.84 (5.85)	8.56 (8.51)	9.69 (9.71)	17	199
16	$[Zn(L^3)_2(H_2O)_2]$	$C_{36}H_{38}ZnN_4O_4$	White	656.12 (657.10)	76	65.92 (65.90)	5.83 (5.84)	8.51 (8.54)	9.94 (9.97)	18	195
17	$[Co(L^4)_2(H_2O)_2]$	$C_{32}H_{32}CoN_6O_4$	Reddish brown	625.10 (626.57)	75	61.61 (61.64)	5.15 (5.17)	13.49 (13.48)	9.43 (9.45)	15	215
18	$[Ni(L^4)_2(H_2O)_2]$	$C_{32}H_{32}NiN_6O_4$	Green	625.17 (626.33)	74	61.67 (61.66)	5.20 (5.17)	13.49 (13.48)	9.44 (9.42)	17	245
19	$[Cu(L^4)_2{\cdot}(H_2O)_2]$	$C_{32}H_{32}CuN_6O_4$	Brown	628.15 (629.45)	77	61.20 (61.18)	5.15 (5.13)	13.37 (13.38)	10.14 (10.12)	18	225
20	$[Zn(L^4)_2(H_2O)_2]$	$C_{32}H_{32}ZnN_6O_4$	White	630.05 (631.15)	79	61.03 (61.00)	5.14 (5.12)	13.33 (13.34)	10.40 (10.38)	19	231

acetates at constant stirring in molar ratio 2:1. All the compounds were soluble in MeOH, $CDCl_3$ and DMSO but were insoluble in water. The hydrazones and transition metal complexes (1–20) were characterized by various spectroscopic techniques (NMR, Mass, FT-IR, ESR, electronic, fluorescence), which suggests octahedral geometry of complexes formulated as $[M(L^{1-4})_2(H_2O)_2]$ where hydrazones get bonded to metal centre through the nitrogen of (C=N) and oxygen of carbonyl group in enolic form. The compounds were stable in air, differently coloured solid, obtained in good yield and non-electrolytic in nature as their molar conductance values are in range 11–20 $\Omega^{-1}cm^2mol^{-1}$ [31]. The analytical data are depicted in experimental part and in Table 1 given in supplementary data.

$$M(CH_3COO)_2 \cdot xH_2O + HL^{1-4} \rightarrow [M(L^{1-4})_2(H_2O)_2] + 2CH_3COOH$$

where M = Co(II), Ni(II), Cu(II) and Zn(II).

IR spectra of compounds

The FT-IR spectral analysis of compounds was obtained in 400–4000 cm^{-1} region by using KBr pellets. The bands of hydrazones and their respective complexes tabulated in Table 2 given in supplementary data and experimental part were compared with each other to confirm the coordination sites on the basis of the shifts in the

Table 2 Characteristic IR frequencies $\nu(cm^{-1})$ of hydrazones and their respective transition metal(II) complexes

C. no.	Compounds	ν(–HOH) water	ν(C=O) amide	ν(–C=N)	ν(N–H)	ν(N–N–H)	ν(M–O)	ν(M–N)
1	HL^1	–	1653	1615	3258	1013	–	–
2	HL^2	–	1648	1612	3242	1011	–	–
3	HL^3	–	1645	1610	3246	1015	–	–
4	HL^4	–	1655	1613	3248	1018	–	–
5	$[Co(L^1)_2(H_2O)_2]$	3427	–	1598	–	1017	545	435
6	$[Ni(L^1)_2(H_2O)_2]$	3425	–	1594	–	1021	547	440
7	$[Cu(L^1)_2(H_2O)_2]$	3428	–	1595	–	1023	543	442
8	$[Zn(L^1)_2(H_2O)_2]$	3430	–	1586	–	1029	548	439
9	$[Co(L^2)_2\cdot(H_2O)_2]$	3417	–	1591	–	1016	540	426
10	$[Ni(L^2)_2(H_2O)_2]$	3415	–	1588	–	1017	542	422
11	$[Cu(L^2)_2(H_2O)_2]$	3422	–	1589	–	1018	539	425
12	$[Zn(L^2)_2(H_2O)_2]$	3425	–	1585	–	1019	537	427
13	$[Co(L^3)_2(H_2O)_2]$	3431	–	1599	–	1021	547	434
14	$[Ni(L^3)_2(H_2O)_2]$	3434	–	1590	–	1023	540	435
15	$[Cu(L^3)_2(H_2O)_2]$	3437	–	1591	–	1025	554	437
16	$[Zn(L^3)_2(H_2O)_2]$	3435	–	1592	–	1024	550	431
17	$[Co(L^4)_2(H_2O)_2]$	3437	–	1588	–	1024	545	442
18	$[Ni(L^4)_2\cdot(H_2O)_2]$	3440	–	1584	–	1021	546	436
19	$[Cu(L^4)_2(H_2O)_2]$	3448	–	1593	–	1026	543	440
20	$[Zn(L^4)_2(H_2O)_2]$	3446	–	1596	–	1025	547	445

absorbance frequency of different types of groups and the absence of certain absorption band due to changes in the electronic environment of the hydrazones after complexation. A strong band in ligands at 1615–1610 cm^{-1} due to azomethine group shifts to the lower-frequency region 1599–1584 cm^{-1} on complexation with the metal atom; this downfield shifting shows the bonding via lone pair of the nitrogen of (C=N) group to metal centre [32, 33]. The bands in the region 1655–1645 cm^{-1} due to υ(C=O) group and at 3258–3242 cm^{-1} due to υ(N–H) group in Schiff base hydrazones got disappeared, indicating their enolization and chelation with metal centre. The shifting of υ(N–N-H) band at 1018–1011 cm^{-1} in free hydrazone to higher value 1029–1016 cm^{-1} in the transition metal complexes confirmed the coordination via lone pair electron of the nitrogen to the metal centre. The appearance of new sharp and distinct bands in the far-infrared spectra of all complexes at 554–537 cm^{-1} and 445–422 cm^{-1}, due to M–O and M–N bonds, suggests the coordination of metal with oxygen and nitrogen atoms [34]. A broad peak near 3448–3415 cm^{-1} is due to stretching vibration of water molecules coordinated to the central metal ion [35]. From the above IR data, it is suggested that hydrazones are bidentate (NO) in nature, and they bind with the metal ion through a nitrogen of (C=N) group and oxygen of carbonyl group.

NMR spectra of compounds

^{1}H NMR spectra

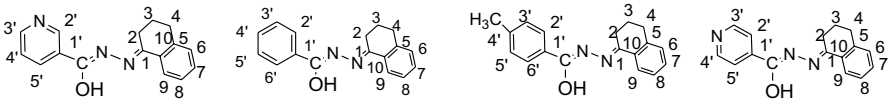

HL^1 HL^2 HL^3 HL^4

NMR spectra of hydrazones and their zinc(II) complexes were obtained in $CDCl_3$, and their δ values are presented in "experimental" section and Table 3 given in supplementary data**.** The binding sites (NO) of the hydrazones were confirmed by correlating spectra of ligands with respective zinc complexes. The hydrazones (1–4) exhibit a singlet at δ 9.86–8.88 ppm due to (–NH) proton which gets disappeared upon complexation, and the proton loss on the nitrogen indicated deprotonation of –NH group due to the presence of keto-enol tautomerism on coordination with the transition metal ion. The metal binds through nitrogen of (C=N) and oxygen of deprotonated carbonyl oxygen in enolized form showing bidentate nature of hydrazones, which was also supported with the IR spectra results [36]. The aromatic protons were recognized in the range δ 8.78–7.06 ppm, which exhibits only minor change in the complexes as a result of binding with the metal ion [37]. A sharp singlet of the three hydrogen atoms of the methyl group at 2.45 ppm in HL^3 ligand remains almost unaltered on complexation. The signals due to CH_2 group of

Table 3 ^{1}H and ^{13}C NMR spectral data (δ in ppm) of the hydrazones and their Zn(II) complexes

Compounds	^{1}H NMR ($CDCl_3$) δ in ppm	^{13}C NMR ($CDCl_3$) δ in ppm
L^1	9.26 (*s*, *t*, 1H, N=C–OH), 7.85 (*d*, J=9.2 Hz, 1H, C_5'–H), 7.51 (*d*, J=7.6 Hz, 1H, C_9–H), 7.21 (*d*, J=7.2 Hz, 2H, C_6–H), 7.18 (*d*, J=7.2 Hz, J=9.8 Hz, 2H, C_7–H), 8.78 (*s*, 1H, C_2'–H), 7.36 (*t*, J=8.4 Hz, 1H, C_8–H), 7.25 (*t*, J=8.2 Hz, 1H, C_4'–H), 8.30 (*s*, 2H, C_3'–H), 2.85 (*t*, J=6.2 Hz, 2H, C_4–H), 2.71 (*t*, J=5.2 Hz, 2H, C_2–H), 2.04 (*m*, J=6.8 Hz, 2H, C_3–H)	166.38 (HNC=O), 151.70 (C_1), 139.66 (C_2'), 131.95 (C_5'), 129.94 (C_9), 137.92 (C_5), 122.92 (C_4'), 133.90 (C_3'), 133.60 (C_1'), 128.93 (C_8), 126.61 (C_6), 124.21 (C_7), 120.12 (C_{10}), 29.93 (C_4), 24.58 (C_2), 21.27 (C_3)
L^2	9.01 (*s*, ^{1}H, N=C–OH), 8.38 (*s*, 1H, C_9–H), 7.89 (*d*, 2H, J=12 Hz, C_2'–H and C_6'–H), 7.59 (*t*, J=7.2 Hz, 1H, C_4'–H), 7.52 (*t*, J=7.6 Hz, 2H, C_3'–H and C_5'–H), 7.28 (*d*, 1H, C_8–H. J=9.6 Hz), 7.16 (*d*, J=7.6 Hz,2H, C_6–H and C_7–H), 2.85 (*t*, J=6 Hz, 2H, C_4–H), 2.68 (*t*, J=5.2 Hz, 2H, C_2–H), 2.03 (*m*, J=6.4 Hz, 2H, C_3–H)	161.31 (HNC=O), 150.62 (C_1), 139.63 (C_5), 135.93 (C_1'), 128.12 (C_9), 131.27 (C_2'), 129.17 (C_6'), 133.61 (C_4'), 130.59 (C_3'), 127.88 (C_5'), 126.61 (C_8), 125.55 (C_6), 125.25 (C_7), 121.18 (C_{10}), 29.62 (C_4), 25.25 (C_2), 21.61 (C_3)
L^3	9.04 (*s*, ^{1}H, N=C–OH), 8.37 (*s*, 1H, C_9–H), 7.31 (*d*, J=8.4 Hz, 2H, C_2'–H and C_6'–H), 7.28 (*d*, J=7.2 Hz, 2H, C_3'–H and C_5'–H), 7.81 (*t*, J=9.2 Hz, 1H, C_8–H), 7.16 (*d*, J=7.6 Hz, 2H,C_6–H and C_7–H), 2.85 (*t*, J=6.0 Hz, 2H, C_4–H), 2.67 (*t*, J=5.2 Hz, 2H, C_2–H), 2.04 (*m*, J=6.8 Hz, 2H, C_3–H), 2.45 (*s*, 3H, $-CH_3$)	163.63 (HNC=O), 153.64 (C_1), 139.92 (C_5), 132.54 (C_1'), 130.20, (C_9), 127.90 (C_2'), 126.23 (C_6'), 133.58 (C_4'), 128.56 (C_3'), 127.58 (C_5'), 126.91 (C_8), 124.57 (C_6), 123.88 (C_7), 122.24 (C_{10}), 29.62 (C_4), 23.29 ($-CH_3$), 25.17 (C_2), 21.58 (C_3)
L^4	9.86 (*s*, ^{1}H, N=C–OH), 8.24 (*s*, 1H, C_9–H), 7.66 (*d*, J=9.2 Hz, 2H, C_2'–H and C_5'–H), 8.67 (*d*, J=15.6 Hz, 2H, C_3'–H and C_4'–H), 7.06 (*t*, J=6.2 Hz, 1H, C_8–H), 7.16 (*d*, J=5.8 Hz, 2H, C_6–H and C_7–H), 2.85 (*t*, J=6.2 Hz, 2H, C_4–H), 2.71 (*t*, J=5.2 Hz, 2H, C_2–H), 2.04 (*m*, J=6.8 Hz, 2H, C_3–H)	162.37 (HNC=O), 147.15 (C_1), 142.99 (C_5), 133.22(C_1'), 126.85(C_9), 128.55 (C_2'), 131.26 (C_3'), 130.22 (C_4'), 128.23 (C_5'), 129.24 (C_8), 127.20 (C_6), 123.90 (C_7), 121.17 (C_{10}), 29.61 (C_4), 26.79(C_2), 21.58 (C_3)
$[Zn(L^1)_2(H_2O)_2]$	7.85 (*d*, J=9.2 Hz, 1H, C_5'–H), 7.51 (*d*, J=7.6 Hz, 1H, C_9–H), 8.52 (*d*, J=7.6 Hz, 1H, C_2'–H), 7.25 (*t*, J=8.2 Hz, 1H, C_4'–H), 8.07 (*s*, 2H, C_3'–H), 7.35 (*t*, J=8.4 Hz, 1H, C_8–H), 7.21 (*d*, J=7.2 Hz, 2H, C_6–H), 7.18 (*d*, J=7.2 Hz, 2H, C_7–H), 2.86 (*t*, J=6.2 H, 2H, C_4–H), 2.70 (*t*, J=5.2 Hz, 2H, C_2–H), 2.44 (*s*, 2H, H_2O), 2.04 (*m*, J=6.8 Hz, 2H, C_3–H)	169.02 (N=C–OH), 152.79 (C_1), 139.60 (C_2'), 131.93 (C_5'), 129.84 (C_9), 137.94 (C_5), 122.92 (C_4'), 133.91 (C_3'), 133.62 (C_1'), 128.97 (C_8), 126.62 (C_6), 124.22 (C_7), 120.16 (C_{10}), 29.96 (C_4), 24.23 (C_2), 21.35(C_3)

Table 3 (continued)

Compounds	^{1}H NMR ($CDCl_3$) δ in ppm	^{13}C NMR ($CDCl_3$) δ in ppm
$[Zn(L^4)_2(H_2O)_2]$	8.32 (*d*, 1H, C_9–H), 7.88 (*d*, *J* = 12, Hz 2H, C_2'–H and C_6'–H), 7.61 (t, J = 7.2 Hz, 1H, C_4'–H), 7.52 (t, J = 7.6 Hz, 2H, C_3'–H and C_5'–H), 7.28 (d, J = 9.2 Hz, 1H, C_8–H), 7.16 (d, J = 7.6 Hz, 2H, C_6–H and C_7–H), 2.84 (t, J = 6 Hz, 2H, C_4–H), 2.68 (t, J = 5.4 Hz, 2H, C_2–H), 2.03 (m, J = 6.4 Hz, 2H, C_3–H), 2.40 (s, 2H, H_2O)	164.02 (N=C–OH), 153.63(C_1), 142.26 (C_5), 135.95(C_1'), 128.54 (C_9), 131.94 (C_2'), 129.91 (C_6'), 133.23 (C_4'), 130.60 (C_3'), 127.58 (C_4'), 126.61 (C_8), 125.55 (C_6), 125.25 (C_7), 121.19 (C_{10}), 29.63 (C_4), 25.23 (C_2), 20.28 (C_3)
$[Zn(L^4)_2(H_2O)_2]$	8.21(*d*, *J* = 8 Hz, 1H, C_9–H), 7.30 (*t*, *J* = 8.4 Hz, 1H, C_4'–H and C_2'–H), 7.28 (*d*, *J* = 7.2 Hz, 2H, C_3'–H and C_5'–H), 7.62 (*t*, *J* = 7.6 Hz, 1H, C_8–H), 7.16 (*d*, *J* = 7.6 Hz, 2H, C_6–H and C_7–H), 2.85 (*t*, *J* = 6.2 Hz, 2H, C_4–H), 2.67 (*t*, *J* = 5.2 Hz, 2H, C_2–H), 2.03 (*m*, *J* = 6.8 Hz, 2H, C_3–H), 2.46 (*s*, 3H, $-CH_3$), 2.38 (*s*, 2H, H_2O)	165.37 (N=C–OH), 154.62 (C_1), 143.61 (C_5), 132.54 (C_1'), 130.20, (C_9), 127.90 (C_2'), 126.23 (C_6'), 133.58 (C_4'), 128.56 (C_3'), 129.74 (C_4'), 127.98 (C_5'), 126.91 (C_8), 124.44 (C_6), 123.86 (C_7), 122.25 (C_{10}), 29.62 (C_4), 23.19 ($-CH_3$), 25.27 (C_2), 21.58 (C_3)
$[Zn(L^4)_2(H_2O)_2]$	8.03 (*s*, *J* = 9.2 Hz, 1H, C_9–H), 7.66 (*d*, *J* = 9.2 Hz, 2H, C_2'–H and C_5'–H), 8.66 (*d*, *J* = 15.2 Hz, 2H, C_3'–H and C_4'–H), 7.06 (*t*, *J* = 7.2 Hz, 1H, C_8–H), 7.16 (*d*, *J* = 7.2 Hz, 2H, C_6–H and C_7–H), 2.85 (*t*, *J* = 6.2 Hz, 2H, C_4–H), 2.68 (*t*, *J* = 5.2 Hz, 2H, C_2–H), 2.04 (*m*, *J* = 6.8 Hz, 2H, C_3–H), 2.40 (*s*, 2H, H_2O)	166.34 (N=C–OH), 149.63 (C_1), 142.95(C_5), 133.22(C_1'), 126.85(C_9), 128.55 (C_2'), 131.26 (C_3'), 130.22 (C_4'), 128.23 (C_5'), 129.24 (C_8), 127.20 (C_6), 123.90 (C_7), 121.17 (C_{10}), 29.61 (C_4), 26.31(C_2), 21.28 (C_3)

aliphatic ring protons of C_2, C_3, and C_4 carbon are in the range δ 2.85–2.04 ppm, which stands almost unaltered on complexation.

^{13}C NMR spectra

The ^{13}C NMR spectra of hydrazones showed that characteristic signals at δ 166.38–161.31 ppm due to (HNC=O) carbon, which display upward shifting in the complexes, indicated the coordination of oxygen atom through lone pair electrons of carbonyl group to the metal ion and the upfield shifting of C_1 carbon of (C=N) group from δ 153.64–147.15 to δ 154.62–149.63 ppm reveals the coordination of lone pair of nitrogen to the metal ion centre. The peaks of aromatic carbons in hydrazones were found near δ 142.99–120.12 ppm, which exhibited only small alteration upon coordination with transition metal ion. The signal due to carbon of ($-CH_3$) in HL^3 ligand was observed near δ 23.29 ppm and remains unaltered upon complexation. The signals at δ 29.93–21.27 ppm due to the aliphatic ring C_2, C_3, and C_4 carbons remain almost unchanged. All peak values (^{1}H NMR and ^{13}C NMR) and their graph related to synthesized ligands and their Zn(II) complexes are given in supplementary data.

Mass spectra of compounds

The mass spectra of the hydrazones and their metal complexes were obtained and are specified in analytical Table 1, and their molecular ion peaks are in agreement with the expected molar weight values. The mass spectrum provides valuable information about the molar weight and structure of compounds. The mass fragmentation of the ligand HL^4 (4) is depicted in Fig. 1 and Scheme 2. The mass spectra show that a molecular ion peak of high intensity at $m/z = 266.1277$ is assigned for $[M+1]^+$, which shows two fragmentation paths where one path shows a peak value at $m/z = 189.1113$ due to loss of pyridine moiety followed by mass spectrum peak at $m/z = 161.0964$ due to loss of CO group and at $m/z = 145.0761$ by loss of NH group. Another fragmentation path depicts peaks at $m/z = 139.0648$ due to loss of pyridine ring and aromatic ring followed by $m/z = 111.0568$ due to loss of CO group.

In the mass spectra of $[Co(L^4)_2(H_2O)_2]$ (17) the molecular ion peak at $m/z = 626.1076$ due to $[M+1]^+$ is observed, which agrees with its molecular weight which are described in Fig. 2. The molecular ion peak obtained at $m/z = 587.1855$ is due to loss of both water molecules coordinated to the transition metal. The peak at m/z 266.1624 is due to loss of one ligand moiety and cobalt metal itself (Scheme 3) and after this complex follows the similar fragmentation pattern as hydrazone HL^4.

Based upon the above mass spectral results, all the transition metal complexes follow the similar fragmentation model. The molecular ion peaks obtained from mass spectra were found to be in good agreement with the expected values of the elemental analysis. The mass spectra of all the hydrazones and their metal complexes indicate their bidentate nature, and the complexation of hydrazones with central metal atom is in 2:1 ratio with molecular formula $[M(L^{1-4})_2(H_2O)_2]$.

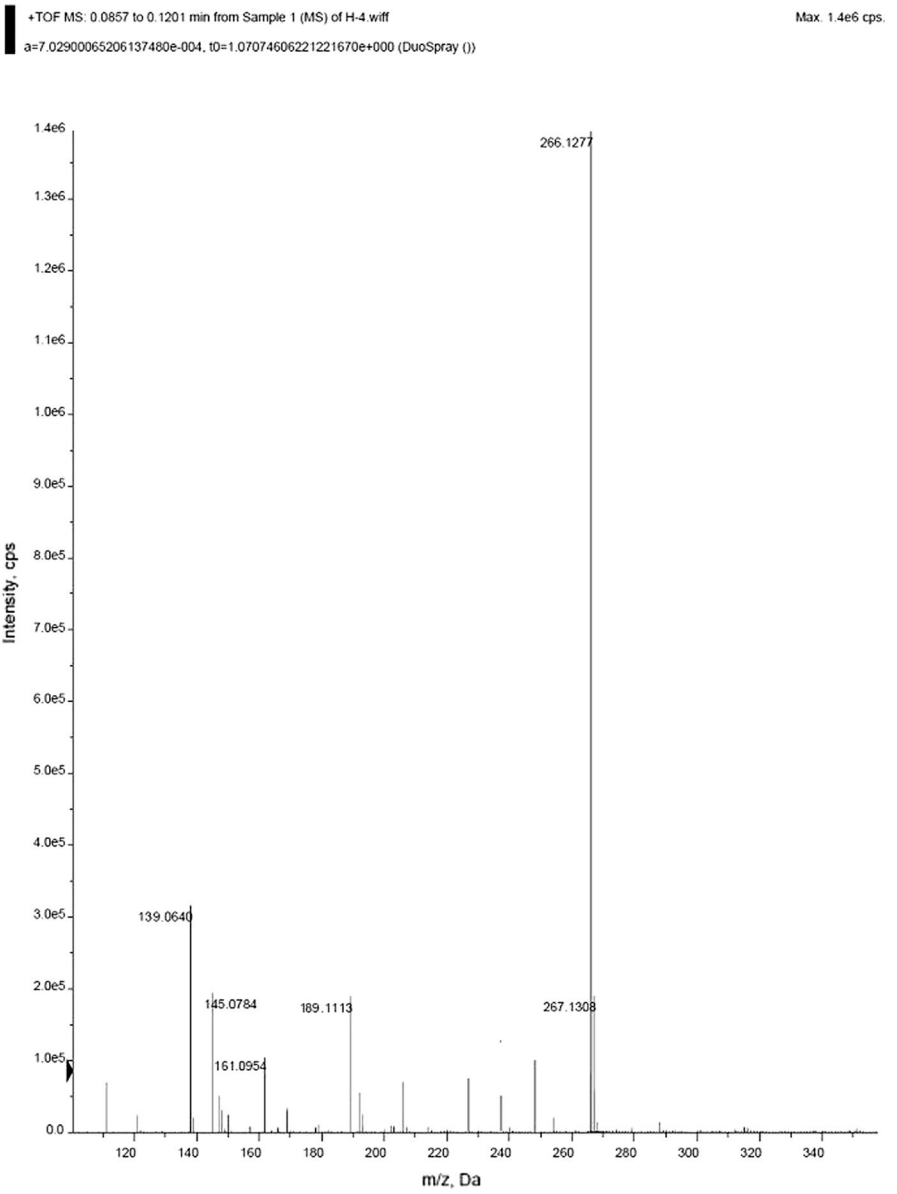

Fig. 1 Mass spectra of hydrazone HL^4 (4)

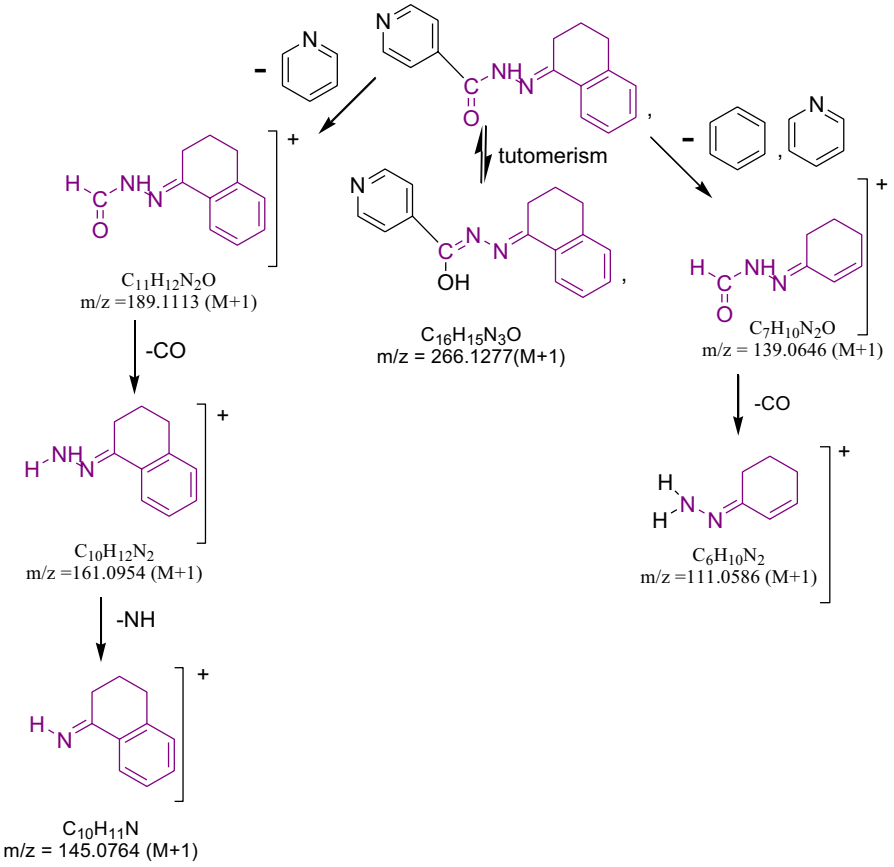

Scheme 2 The possible molecular ion fragmentation pattern from the mass spectrum of hydrazone HL^4 (4)

ESR spectra of compounds

The solid-state ESR analysis of the copper (II) complexes was obtained at RT (300 K) and LNT (77 K) in DMSO to gather information about stereochemistry, bonding nature of ligands and metal ion. From the ESR data, the spin Hamiltonian parameters were determined and are summarized in Table 4. The ESR spectrum of $[Cu(L^3)_2(H_2O)_2]$ (15) complex describes a strong band in the upfield region, which may be due to tumbling. The trend followed for g tensor values was: $g_{\|}$ (2.43) > $g_{\perp}$(2.14) > g_c(2.0023), suggesting residence of single unpaired electron in the $d_{x^2-y^2}$ orbital of Cu(II) ions in the ground state [38], which is predictable feature of octahedral geometry around metal ions and g_{av} was obtained by the formula: 1/3

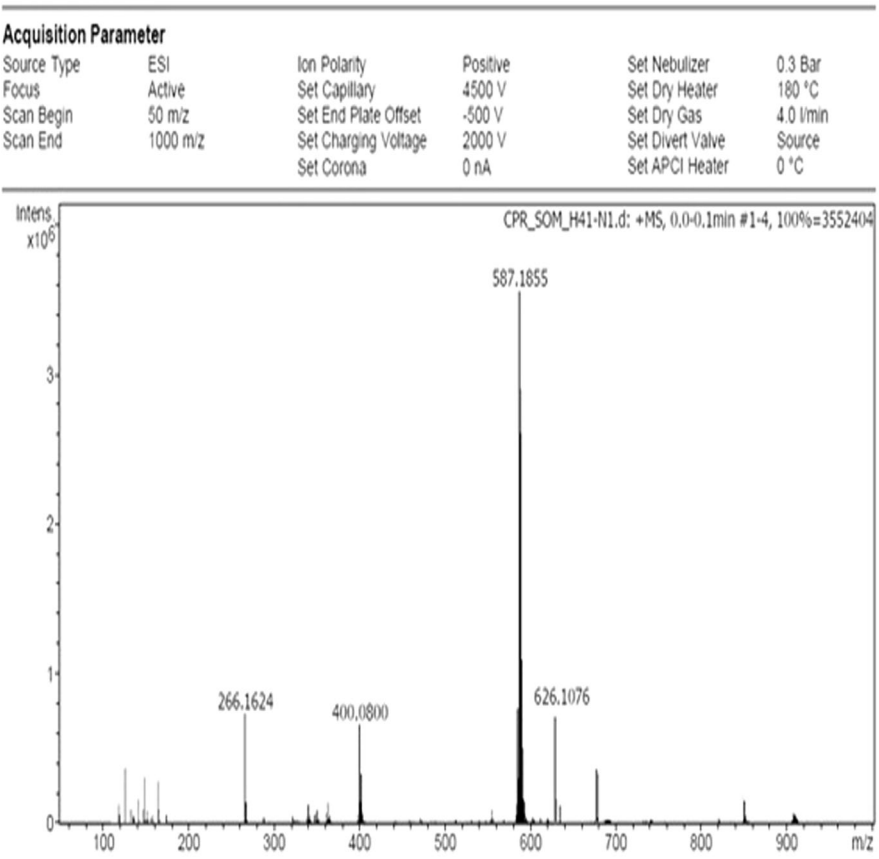

Fig. 2 Mass spectra of $[Co(L^4)_2(H_2O)_2]$ (17)

($g_{||}+2\ g_{\perp}$) which were found to be lower than free copper(II) ion λ (832 cm^{-1}). Spin orbital coupling constant λ is calculated from relation $g_{av}=2(1-2\ \lambda/10Dq)$, and it supports the evidence for metal → ligand bond to be covalent in nature, and this was also confirmed from g_{av} values (2.23) of the complex and the spectral parameters of Cu(II) complexes are given in Table 4.

The measured anisotropic geometric parameter G and g tensor values indicate the exchange interactions among the copper(II) ion and may be calculated by utilizing the subsequent equation $G=(g_{||}-2.0023)/(g_{\perp}-2.0023)$ [39]. If $G<4$, then different types of exchange interactions among the Cu(II) centre are present, and if $G>4$, then these exchange interactions were minor. In all these copper complexes, the G

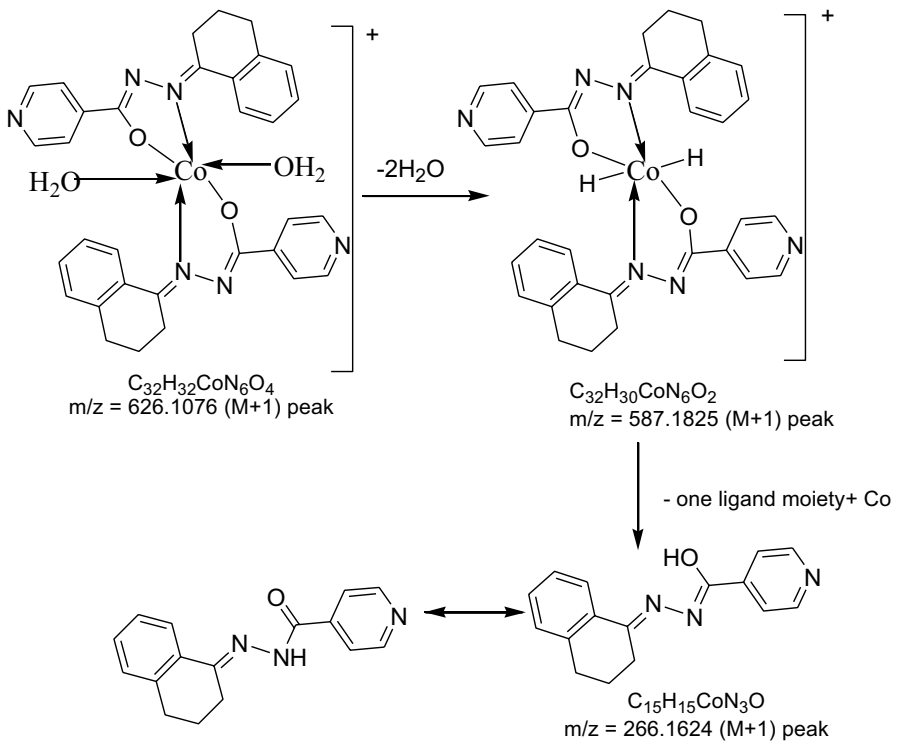

Scheme 3 The possible molecular ion fragmentation pattern for the complex $[Co(L^4)_2(H_2O)_2]$ (17)

values were found to be in range 2.96–3.69, indicative of considerable exchange interactions among the Cu(II) centres in the solid steady state [40].

Electronic spectra of compounds

The electronic spectra of the compounds were carried out in solvent DMSO, and their band assignments are given in Table 5. The electronic spectra of free hydrazones showed a band at 28,278–29,815 cm^{-1} and 31,673–33,745 cm^{-1} attributed to $n \rightarrow \pi^*$ and $\pi \rightarrow \pi^*$ transitions. Shifting in the value of $n \rightarrow \pi^*$ transition shows

Table 4 ESR spectral parameters of Cu(II) complexes

Cu(II) complexes	$g_{\parallel}$	$g_{\perp}$	g_{av}	G
$[Cu(L^1)_2(H_2O)_2]$	2.40	2.11	2.20	3.69
$[Cu(L^2)_2(H_2O)_2]$	2.43	2.14	2.23	3.10
$[Cu(L^3)_2(H_2O)_2]$	2.41	2.12	2.21	3.46
$[Cu(L^4)_2(H_2O)_2]$	2.44	2.15	2.24	2.96

Table 5 Electronic spectral data and magnetic moment (BM) of hydrazones and their transition metal(II) complexes

Compounds	Ligand/Complex	Band assignment	Transitions	μ_{eff}(BM)	Geometry
1	$[HL^1]$	31,698	$\pi \rightarrow \pi^*$	–	–
		29,247	$n \rightarrow \pi^*$		
2	$[HL^2]$	31,673	$\pi \rightarrow \pi^*$	–	–
		28,278	$n \rightarrow \pi^*$		
3	$[HL^3]$	33,745	$\pi \rightarrow \pi^*$	–	–
		29,815	$n \rightarrow \pi^*$		
4	$[HL^4]$	32,689	$\pi \rightarrow \pi$	–	–
		29,231	$n \rightarrow \pi^*$		
5	$[Co(L^1)_2(H_2O)_2]$	23,531	$^4T_{1g}(F) \rightarrow {}^4T_{1g}(P)$ (ν_1)	4.70	Octahedral
		17,745	$^4T_{1g}(F) \rightarrow {}^4A_{2g}(F)$ (ν_2)		
		9577	$^4T_{1g}(F) \rightarrow {}^4T_{2g}(F)$ (ν_3)		
6	$[Ni(L^1)_2(H_2O)_2]$	24,345	$^3A_{2g}(F) \rightarrow {}^3T_{2g}(F)$ (ν_1)	3.00	Octahedral
		18,332	$^3A_{1g}(F) \rightarrow {}^3T_{1g}(F)$ (ν_2)		
		10,467	$^3A_{2g}(F) \rightarrow {}^3T_1g(P)$ (ν_3)		
7	$[Cu(L^1)_2(H_2O)_2]$	24,156	$^2B_{1g} \rightarrow {}^2A_{1g}$ (ν_1)	1.91	Octahedral
		15,823	$^2B_{1g} \rightarrow {}^2E_{2g}$ (ν_2)		
8	$[Zn(L^1)_2(H_2O)_2]$	24,456	LMCT	–	Octahedral
9	$[Co(L^2)_2(H_2O)_2]$	23,423	$^4T_{1g}(F) \rightarrow {}^4T_{1g}(P)$ (ν_1)	4.60	Octahedral
		17,734	$^4T_{1g}(F) \rightarrow {}^4A_{2g}(F)$ (ν_2)		
		9455	$^4T_{1g}(F) \rightarrow {}^4T_{2g}(F)$ (ν_3)		
10	$[Ni(L^2)_2(H_2O)_2]$	24,291	$^3A_{2g}(F) \rightarrow {}^3T_{2g}(F)$ (ν_1)	2.80	Octahedral
		18,226	$^3A_{1g}(F) \rightarrow {}^3T_{1g}(F)$ (ν_2)		
		10,453	$^3A_{2g}(F) \rightarrow {}^3T_{1g}(P)$ (ν_3)		
11	$[Cu(L^2)_2(H_2O)_2]$	24,042	$^2B_{1g} \rightarrow {}^2A_{1g}$ (ν_1)	1.78	Octahedral
		15,618	$^2B_{1g} \rightarrow {}^2E_{2g}$ (ν_2)		
12	$[Zn(L^2)_2(H_2O)_2]$	24,440	LMCT	–	Octahedral
13	$[Co(L^3)_2(H_2O)_2]$	23,649	$^4T_{1g}(F) \rightarrow {}^4T_{1g}(P)$ (ν_1)	5.00	Octahedral
		17,861	$^4T_{1g}(F) \rightarrow {}^4A_{2g}(F)$ (ν_2)		
		9587	$^4T_{1g}(F) \rightarrow {}^4T_{2g}(F)$ (ν_3)		
14	$[Ni(L^3)_2(H_2O)_2]$	24,675	$^3A_{2g}(F) \rightarrow {}^3T_{2g}(F)$ (ν_1)	3.30	Octahedral
		18,645	$^3A_{1g}(F) \rightarrow {}^3T_{1g}(F)$ (ν_2)		
		10,582	$^3A_{2g}(F) \rightarrow {}^3T_{1g}(P)$ (ν_3)		
15	$[Cu(L^3)_2(H_2O)_2]$	24,272	$^2B_{1g} \rightarrow {}^2A_{1g}$ (ν_1)	1.95	Octahedral
		15,847	$^2B_{1g} \rightarrow {}^2E_{2g}$ (ν_2)		
16	$[Zn(L^3)_2(H_2O)_2]$	24,468	LMCT	–	Octahedral
17	$[Co(L^4)_2(H_2O)_2]$	23,527	$^4T_{1g}(F) \rightarrow {}^4T_{1g}(P)$ (ν_1)	4.90	Octahedral
		17,844	$^4T_{1g}(F) \rightarrow {}^4A_{2g}(F)$ (ν_2)		
		9575	$^4T_{1g}(F) \rightarrow {}^4T_{2g}(F)$ (ν_3)		
18	$[Ni(L^4)_2(H_2O)_2]$	24,437	$^3A_{2g}(F) \rightarrow {}^3T_{2g}(F)$ (ν_1)	3.20	Octahedral
		18,429	$^3A_{1g}(F) \rightarrow {}^3T_{1g}(F)$ (ν_2)		
		10,664	$^3A_{2g}(F) \rightarrow {}^3T_1g(P)(\nu_3)$		

Table 5 (continued)

Compounds	Ligand/Complex	Band assignment	Transitions	μ_{eff}(BM)	Geometry
19	$[Cu(L^4)_2(H_2O)_2]$	24,214	$^2B_{1g} \rightarrow {}^2A_{1g}$ (v_1)	1.85	Octahedral
		15,720	$^2B_{1g} \rightarrow {}^2E_{2g}$ (v_2)		
20	$[Zn(L^4)_2(H_2O)_2]$	24,450	LMCT	–	Octahedral

the complexation of metal ion with hydrazones and the transitions due to aromatic carbon ($\pi \rightarrow \pi^*$) remains unaltered. The spectra of the $[Co(L^{1-4})_2(H_2O)_2]$ complexes exhibit three d–d absorption transitions in the range 23,423–23,649 cm^{-1}, 17,734–17,861 cm^{-1}, and 9455–9587 cm^{-1} due to $^4T_{1g}(F) \rightarrow {}^4T_{1g}(P)$, $^4T_{1g(}F) \rightarrow {}^4A_{2g}(F)$ and $^4T_{1g}(F) \rightarrow {}^4T_{2g}(F)$ transitions which suggests octahedral geometry of cobalt(II) complexes [41].

The ESR graph is depicted in Fig. 3 at room temperature and liquid nitrogen temperature.

The spectra of $[Ni(L^{1-4})_2(H_2O)_2]$ complexes showed three d-d absorption transitions in the range of 24,291–24,675 cm^{-1}, 18,226–18,645 cm^{-1} and 10,453–10,582 cm^{-1}, ascribed to the $^3A_{2g}(F) \rightarrow {}^3T_{1g}(P)$, $^3A_{1g}(F) \rightarrow 3T_{1g}(F)$ and $^3A_{2g}(F) \rightarrow {}^3T_{2g}(F)$ transitions, respectively, which results in the octahedral geometry of nickel(II) ions [42]. The spectra of $[Cu(L^{1-4})_2(H_2O)_2]$ complexes showed two absorption transitions at 24,042–24,272, 15,618–15,847 cm^{-1} assigned to $^2B_{1g} \rightarrow {}^2A_{1g}(\nu_1)$ and $^2B_{1g} \rightarrow {}^2E_{2g}$ (ν_2) transitions [43], and spectral data of $[Zn(L^{1-4})_2(H_2O)_2]$ complexes show only one band in the range of 24,440–24,468 cm^{-1} which is attributed to LMCT transitions [44], and these complexes were diamagnetic in nature with complete filled d^{10} configuration. Based upon the above spectral analysis and analytical data, it was confirmed that all the complexes have octahedral arrangement around central metal ion [45].

Magnetic measurement of compounds

The magnetic moment data of Co(II), Ni(II) and Cu(II) complexes were found to be in range of 4.60–5.00 BM, 2.80–3.30 BM and 1.78–1.95 BM, respectively, which shows the paramagnetic nature of all the three types of metal complexes. The measured μ_{eff} values are in the range known for six coordinated octahedral geometry [46] and the Zn(II) complexes shows a diamagnetic behaviour.

Fluorescence spectra of compounds

The steady-state fluorescence emission spectral analysis of the hydrazones and their corresponding metal complexes were carried out in $CHCl_3$ with an excitation wavelength of 300 nm at 298 K. On complexation, hydrazones indicate some remarkable changes in fluorescent properties like quenching of spectra, variation in intensity, difference of wavelength in emission bands or emergence of new bands, etc. Hydrazone HL^2 (2) observes broad fluorescent emission band at 407 nm, gets

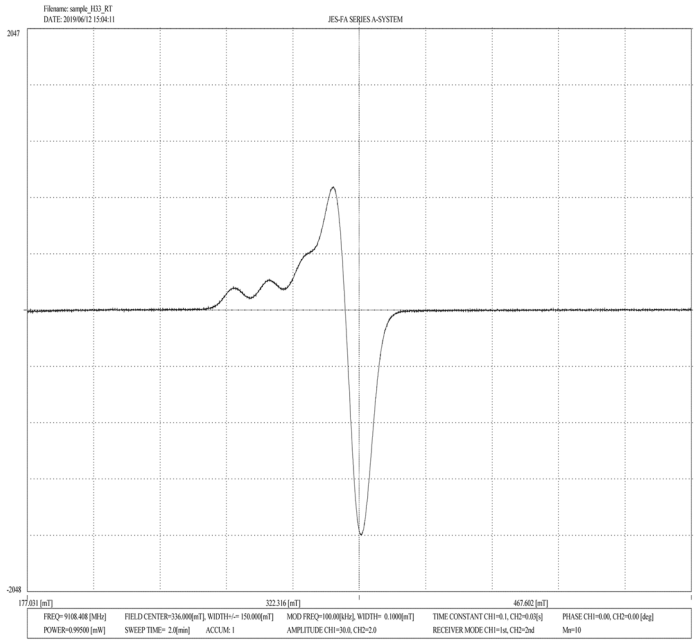

(a)

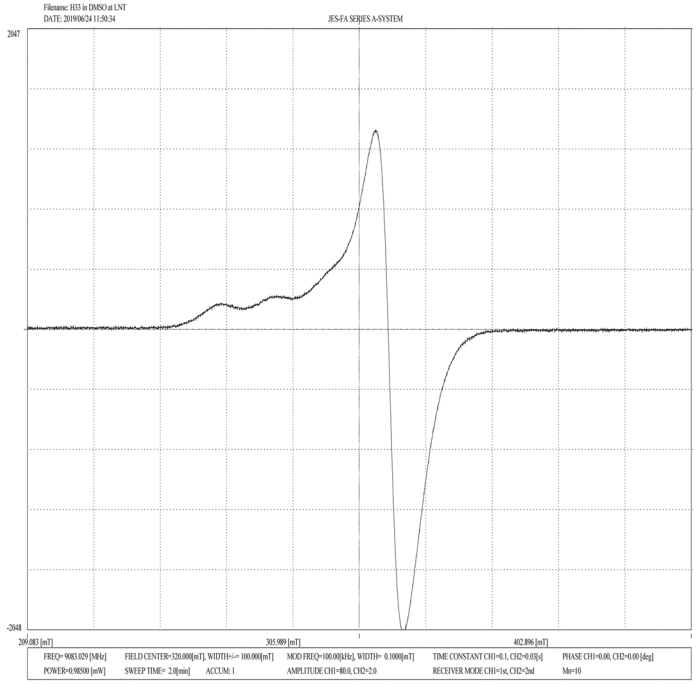

(b)

Fig. 3 ESR spectrum of $[Cu(L^3)_2(H_2O)_2]$(15) at **a** room temperature and **b** liquid nitrogen temperature

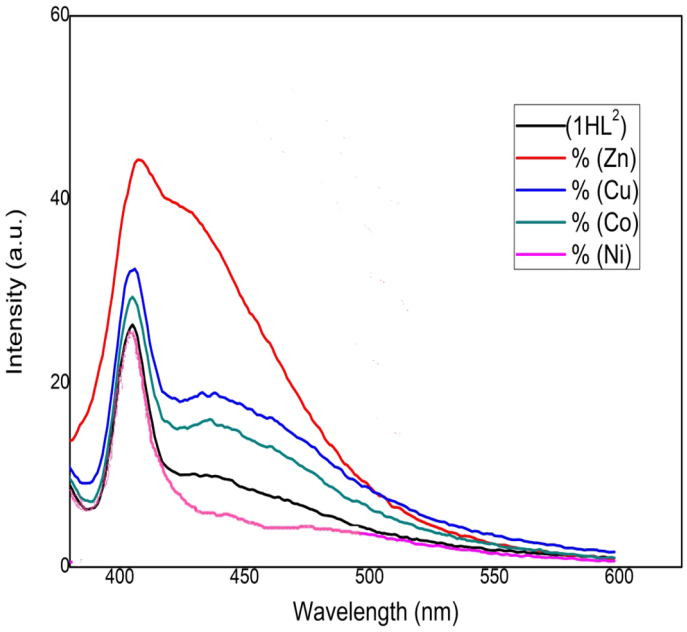

Fig. 4 Fluorescence spectra of hydrazone HL^2 (2) and its transition metal complexes

shifted on coordination with central metal atom and is shown in Fig. 4. The Co(II), Ni(II), Cu(II) and Zn(II) metal complexes that exhibited bands at 410, 408, 412 and 415 nm, respectively, confirm complexation. The intensification in fluorescent spectra (hyperchromic shift) of metal complexes can be ascribed for M → L charge transfer (LMCT) transitions, which showed their extra stability [47]. The order followed for fluorescent properties of hydrazone HL^2 and its metal complexes follows the trend: Zinc(II) > Copper(II) > Cobalt(II) > Nickel(II) > HL^2. The enhancement in fluorescent intensity of zinc complexes is due to their fulfilled d^{10} configuration making them difficult to oxidize and reduce. Based on the above data, it was revealed that the hydrazones and their transition metal complexes are good fluorescent components and may have good photochemical applications [48].

Conductance measurements of compounds

The molar conductance of Co(II), Ni(II), Cu(II) and Zn(II) complexes of 1×10^{-3} M solution is found to be between 11–20 Ω^{-1} cm^{2} mol^{-1}, which confirmed the non-electrolytic nature of compounds [31].

Thermal studies

Thermal behaviour of compounds was analysed by TG/DTA/DTG analysis, and thermal data of the compounds were recorded between temperature 25–550 °C

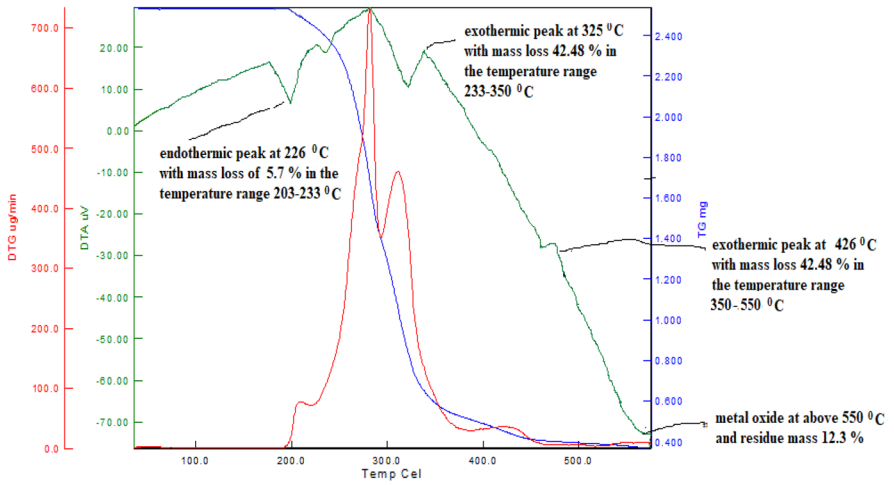

Fig. 5 Thermo gravimetric curve of [Ni $(L^1)_2(H_2O)_2$] (6)

under nitrogen atmosphere with heating rate of 20 °C min^{-1}. In the current study, thermal analysis was carried out to get valuable information about the thermal stability of synthesized complexes and to decide whether water molecules are outside or inside the coordination sphere of metal [49–51]. The various thermal decay steps followed by the complexes with their respective mass loss are presented in Fig. 5. The TG curve of all the complexes follows the same design of three-step decomposition with mass loss till the metal oxide is formed. Thermal analysis describes that the complexes are stable below 180 °C, which indicates that there are no hydrated water molecules of crystallization as no mass loss was noticed up to this temperature, and the first decay step is in the range 180–250 °C revealing the existence of bonded water molecules to central metal atom. The second decay step takes place between the temperature 250 °C and 350 °C with a mass loss attributed to a strong broad exothermic peak on the TG graph agree with thermal decay process of the one hydrazone moiety. The removal of second hydrazone moiety occurs in the range 350–550 °C. The thermal decay of all the transition metal complexes ended with emergence of metal oxide residue[52, 53].

The three-step thermal decay process can be represented as:

[M $(L^{1-4})_2(H_2O)_2$] → [M $(L^{1-4})_2(H_2O)_2$] (no mass loss below 180 °C).

[M $(L^{1-4})_2(H_2O)_2$] → [M $(L^{1-4})_2$] + $2H_2O$ (Decomposition of two water molecules, near 180–250 °C, endothermic peak).

[M $(L^{1-4})_2$] → Intermediate [M (L^{1-4})] (Decomposition of one hydrazone moiety, near 250–350 °C, exothermic peak).

Intermediate → Loss of other hydrazone moiety + metal oxide (Loss of another hydrazone near 350–550 °C, exothermic peak).

Above 550 °C—metal oxide as a residue.

where M = Co(II), Ni(II), Cu(II) and Zn(II).

The TG curve of the Ni(II) complex (6) (Fig. 5) revealed three thermal decay stages in the range 193 to 560 °C and complex is highly stable up to 203 °C, which indicates the absence of hydrated water molecules. The first stage indicates a mass loss of 5.7% (calculated 5.4%) in range 203–233 °C (DTG), which is due to the removal of two H_2O molecules with an endothermic peak at 226 °C. The second stage takes place in the temperature range 233–350 °C with a mass loss of 42.18% (calculated 42.02%) with the appearance of a strong broad exothermic peak exactly at 325 °C. DTA and DTG curve reveal the thermal decay of one hydrazone moiety. In the third stage, dropping of second hydrazone moiety occurs in this temperature interval 350–550 °C with a fall in mass of 42.18% (calculated 42.02%) with the appearance of a strong broad exothermic peak exactly at 426 °C leaving nickel oxide as residue at the end of thermal decay process [54]. The residual mass (12.3%) is presumed to be nickel(II) oxide.

Biological studies

Antimicrobial activity

Hydrazones (HL^{1-4}), their chelated transition metal complexes and standard drugs were evaluated for antimicrobial activity (in vitro) using a serial dilution method against two gram-positive bacteria (*S. aureus, B. subtilis*), 2 g negative bacteria (*E. coli, P. aeruginosa*) and two fungal species (*C. albicans, A.* niger). Ciprofloxacin and fluconazole drugs were used as a positive control for antibacterial and antifungal activities, whereas DMSO is used as negative control having negligible inhibitory effect. Minimum inhibitory concentration (MIC) in µmol/mL is depicted in Table 6 and its charted form is in Fig. 6.

Conclusion drawn from the biological data is summarized below:

1. The order of antimicrobial activity for hydrazones (HL^{1-4}) was found as $HL^3 > HL^1 > HL^4 > HL^2$, which is explained on the basis of nature of compounds [55]. The antimicrobial evaluation of hydrazones is ascribed to the existence of the azomethine (–C=N–) group, which have fine chelating abilities, which results in construction of hydrogen bond with the active centres of the cell constituents, which results in hindrance of normal life process [56]. The presence of electron releasing methyl groups in hydrazone HL^3 makes it highly active.
2. In antibacterial activity, complexes 15, 16, 19 having MIC values in the range 0.0091–0.0317 µmol/mL were found to be more or equally active than standard ciprofloxacin (MIC = 0.0188 µmol/mL) with tested strains of bacteria. Among gram-positive bacteria, complexes were more active towards *B. subtilis* than *S. aureus* and for gram-negative bacteria complexes were more active for *P. aeruginosa* as compared to *E. coli*, and overall results show that compounds show more potency for gram-negative bacteria than gram-positive bacteria due to their distinctive structure and thin cell wall [57, 58].

Table 6 Results of in vitro antimicrobial screening for hydrazones (1–4), mononuclear metal complexes (5–20), and standard drugs (21, 22). (MIC in µmol/mL)

C. no.	Compounds	MIC in µmol/mL					
		Gram-positive bacteria		Gram-negative bacteria		Fungi	
		S. aureus	*B. subtilis*	*E. coli*	*P. aeruginosa*	*C. albicans*	*A. niger*
1	HL^1	0.0942	0.1885	0.1885	0.1885	0.1885	0.0942
2	HL^2	0.1892	0.1892	0.1892	0.0946	0.1892	0.1892
3	HL^3	0.0850	0.0425	0.1700	0.0425	0.0850	0.1700
4	HL^4	0.1885	0.0942	0.1885	0.1885	0.1885	0.1885
5	$[Co(L^1)_2(H_2O)_2]$	0.0800	0.0800	0.0400	0.0800	0.0800	0.0800
6	$[Ni(L^1)_2(H_2O)_2]$	0.0797	0.0399	0.0797	0.0797	0.0399	0.0797
7	$[Cu(L^1)_2(H_2O)_2]$	0.0795	0.0397	0.0397	0.0795	0.0199	0.0397
8	$[Zn(L^1)_2(H_2O)_2]$	0.0397	0.0794	0.0794	0.0397	0.0794	0.0794
9	$[Co(L^2)_2(H_2O)_2]$	0.0804	0.0804	0.0804	0.0804	0.0402	0.0804
10	$[Ni(L^2)_2(H_2O)_2]$	0.0802	0.0401	0.0802	0.0401	0.0401	0.0802
11	$[Cu(L^2)_2(H_2O)_2]$	0.0797	0.0797	0.0797	0.0399	0.0199	0.0399
12	$[Zn(L^2)_2(H_2O)_2]$	0.0397	0.0795	0.0397	0.0795	0.0397	0.0795
13	$[Co(L^3)_2(H_2O)_2]$	0.0366	0.0366	0.0732	0.0366	0.0366	0.0732
14	$[Ni(L^3)_2(H_2O)_2]$	0.0730	0.0365	0.0730	0.0365	0.0365	0.0730
15	$[Cu(L^3)_2(H_2O)_2]$	0.0182	0.0091	0.0182	0.0091	0.0091	0.0091
16	$[Zn(L^3)_2(H_2O)_2]$	0.0158	0.0158	0.0317	0.0158	0.0158	0.0158
17	$[Co(L^4)_2(H_2O)_2]$	0.0800	0.0400	0.0800	0.0400	0.0400	0.0800
18	$[Ni(L^4)_2(H_2O)_2]$	0.0797	0.0797	0.0797	0.0397	0.0797	0.0797
19	$[Cu(L^4)_2(H_2O)_2]$	0.0199	0.0199	0.0199	0.0158	0.0199	0.0199
20	$[Zn(L^4)_2(H_2O)_2]$	0.0793	0.0397	0.0397	0.0793	0.0397	0.0397
21	Ciprofloxacin	0.0188	0.0188	0.0188	0.0188		
22	Fluconazole	–	–	–	–	0.0204	0.0204

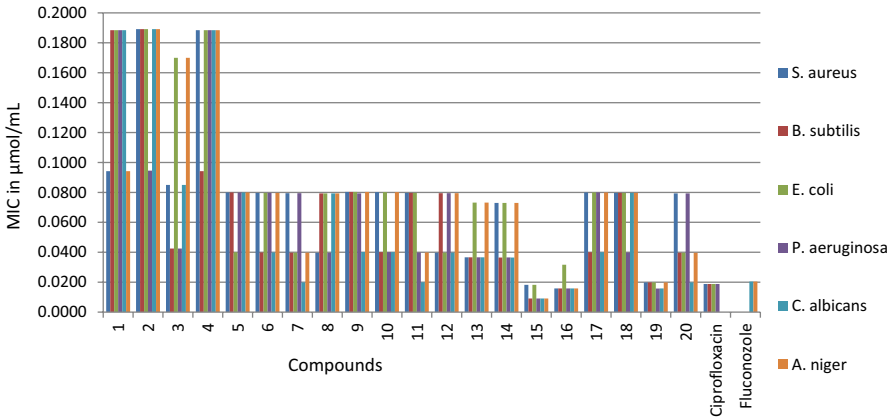

Fig. 6 Graph showing in vitro antimicrobial activity of hydrazones (1–4) and their transition metal complexes (5–20)

3. In case of antifungal activity, complexes 7, 11, 15, 16 and 19 were found to show equally good inhibitory effect than standard fluconazole (MIC = 0.204 µmol/mL) having MIC values in the range 0.0091–0.0399 µmol/mL.

In conclusion, compound (HL^3) and its copper and zinc complexes 15 and 16 are found to more active antimicrobial agent in the entire series of compounds tested. The antibacterial and antifungal evaluation reveals that the transition metal complexes were observed to be more active than their parent hydrazones against same species under similar environmental conditions, and this enhancement is explained by on the basis of overtone's concept of chelation theory as evidenced from literature data [59, 60]. The fluctuations in the antimicrobial study rely on the differences in ribosomes in the microbial cell or the permeability of the cell wall. The lipid membrane surrounding the cell wall favours the movement of any lipid-soluble materials, and it is known that lipid solubility is an major factor to control the antimicrobial activity [61], the nature of metal ion, azomethine linkage in compounds and chelation phenomena that play an effective role in inhibitory activity [62].

Cytotoxicity

Chemotherapy is the branch of science which deals with both localized and metastasized cancers. The compounds (1–20) were tested for their cytotoxic and growth inhibitory activities (in vitro) against three human cancer cell lines (A549, Hela, MCF7) and one normal cell line (L_6) by the MTT assay. Doxorubicin, one of the most active anticancer agents, was taken as a reference standard. The response parameter was determined as the IC_{50} values, which response to the concentration needed for 50% inhibition of cell viability [63, 64]. The correlation between the surviving fraction and drug concentration was plotted to get the survival curve of all the tested cancer cell lines. The trend followed by hydrazones against cell lines is $HL^3 > HL^2 > HL^4 > HL^1$, where HL^3 hydrazone is most active due to electron releasing methyl group attached to benzene ring. In vitro cytotoxicity of the synthesized compounds (1–20) is tabulated in Table 7 and bar graph representation in Fig. 7a–d.

The cytotoxic activity data reveal that:

1. Anticancer activity against human alveolar adenocarcinoma epithelial cell line (A549): Compounds 7 and 15 displayed potent activity, with an IC_{50} value of 13.28 and 12.81 µg/mL. Other compounds 14 and 16 showed good activity with $IC_{50} < 15$ µg/mL, and 3, 8, 9, 11, 12, 13 and 19 gave moderate anticancer activity, while other compounds in the series do not show any activity. The results are summarized in Table 3 and are represented in Fig. 7a.
2. The obtained results for human cervical carcinoma cell line (HeLa) demonstrated that compounds 7, 11 and 15 exhibited very potent activity, with an IC_{50} value of 10.98, 11.05 and 11.82 µg/mL. Other compounds 13, 14 and 15 showed potency with $IC_{50} \leq 15$ µg/mL, whereas 8, 9, 10, 12, 16 and 20 showed moderate anticancer activity, while remaining compounds do not show significant activity. The results are presented in Fig. 7b.

Table 7 Cytotoxicity of hydrazones and their transition metal complexes against three cancer cell lines (A549, Hela, MCF7) and cell line normal (L_6) (IC_{50} = µg/mL)

C. no.	Compounds	Cytotoxicity (IC_{50} = µg/mL)			
		A549	HeLa	MCF7	L_6
1	HL^1	90.50 ± 10.19	98.01 ± 12.54	99.86 ± 10.99	110.41 ± 9.67
2	HL^2	24.32 ± 9.05	35.86 ± 6.76	36.93 ± 11.03	26.61 ± 5.43
3	HL^3	20.32 ± 11.28	24.71 ± 5.80	24.95 ± 4.23	25.37 ± 1.92
4	HL^4	61.34 ± 8.44	63.83 ± 16.42	42.32 ± 9.41	73.56 ± 11.97
5	$[Co(L^1)_2(H_2O)_2]$	90.72 ± 4.18	89.03 ± 10.61	69.48 ± 9.23	105.99 ± 8.91
6	$[Ni(L^1)_2(H_2O)_2]$	26.34 ± 10.54	29.75 ± 11.80	41.48 ± 3.01	34.82 ± 10.39
7	$[Cu(L^1)_2(H_2O)_2]$	13.28 ± 6.49	10.98 ± 6.18	12.41 ± 4.66	16.42 ± 2.72
8	$[Zn(L^1)_2(H_2O)_2]$	18.34 ± 3.89	20.23 ± 2.99	18.51 ± 2.76	36.88 ± 3.95
9	$[Co(L^2)_2(H_2O)_2]$	18.90 ± 4.23	18.94 ± 8.12	19.77 ± 2.04	26.03 ± 2.08
10	$[Ni(L^2)_2(H_2O)_2]$	20.92 ± 8.42	21.58 ± 9.79	30.27 ± 12.36	25.13 ± 14.01
11	$[Cu(L^2)_2(H_2O)_2]$	17.20 ± 3.32	11.05 ± 8.91	15.82 ± 7.23	18.15 ± 12.91
12	$[Zn(L^2)_2(H_2O)_2]$	14.19 ± 2.3	20.19 ± 5.15	30.46 ± 7.08	19.41 ± 8.12
13	$[Co(L^3)_2(H_2O)_2]$	16.4 ± 5.60	14.22 ± 4.12	14.85 ± 3.56	23.51 ± 2.59
14	$[Ni(L^3)_2(H_2O)_2]$	14.24 ± 4.53	13.88 ± 4.46	13.32 ± 3.97	22.91 ± 1.54
15	$[Cu(L^3)_2(H_2O)_2]$	12.81 ± 2.34	11.82 ± 7.35	10.76 ± 3.52	16.30 ± 10.92
16	$[Zn(L^3)_2(H_2O)_2]$	14.24 ± 0.57	21.11 ± 6.74	13.08 ± 10.21	17.42 ± 11.51
17	$[Co(L^4)_2(H_2O)_2]$	50.22 ± 8.34	60.49 ± 5.77	54.30 ± 10.98	71.93 ± 9.07
18	$[Ni(L^4)_2(H_2O)_2]$	36.80 ± 5.21	31.65 ± 5.60	21.89 ± 2.19	24.79 ± 3.15
19	$[Cu(L^4)_2(H_2O)_2]$	27.52 ± 1.14	31.44 ± 6.21	29.69 ± 11.85	38.77 ± 6.41
20	$[Zn(L^4)_2(H_2O)_2]$	20.25 ± 0.19	22.87 ± 13.21	29.29 ± 12.85	41.06 ± 9.30
21	Doxorubicin	0.7 ± 0.11	1.72 ± 0.62	1.95 ± 0.32	2.15 ± 0.95

3. Cytotoxic evaluation against human breast adenocarcinoma cell line (MCF7) shows that complexes 7 and 15 exhibited very good activity, with an IC_{50} value of 12.41 and 10.76 µg/mL. Compounds 13, 14 and 16 were also found to possess potent activity with $IC_{50} \leq 15$ µg/mL, while compounds 8, 9, 11 and 18 showed moderate anticancer activity, and other compounds do not show the activity as shown in Fig. 7c.
4. The cytotoxic potential of the compounds (1–20) against normal cell line (L_6) showed that synthesized compounds were 8–25 times less toxic as compared with the standard drug excluding 1, 4, 5 and 17, which did not induce any toxicity as their IC_{50} values are up to 50 times more than the standard drug. One important aspect for toxicity is that compounds 7 and 15 with IC_{50} value of 16.42 and 16.30 µg/mL were found to be 8 times less toxic than the standard doxorubicin. (IC_{50} value 2.15 µg/mL) against Rat myoblast cell line (L_6), which are highest active against cancer cell lines. The results are presented in Fig. 7d

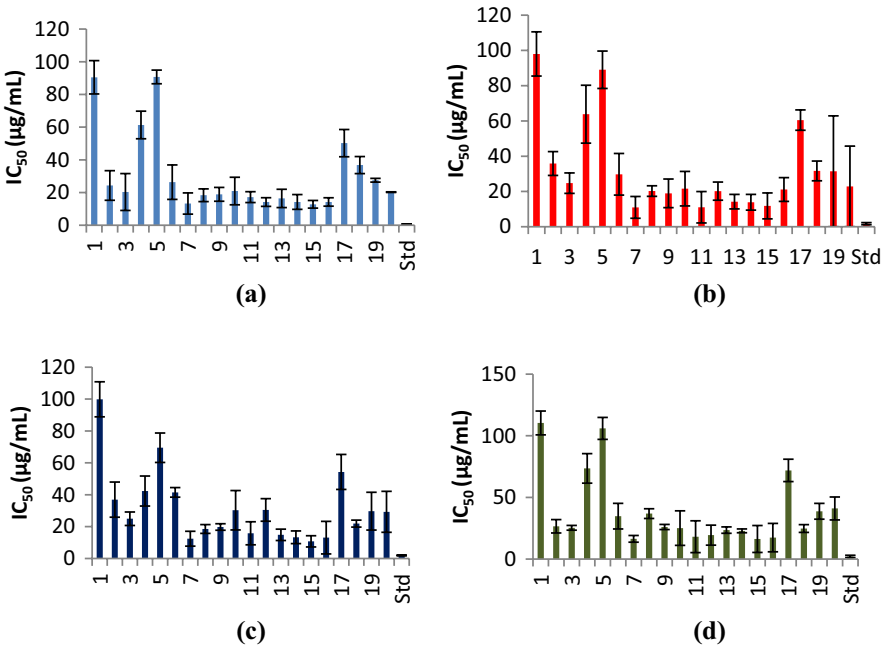

Fig. 7 Anticancer activity of hydrazones and their transition metal complexes showing their IC_{50} values against **a** A549—Human lung carcinoma cell line **b** HeLa—Human cervical carcinoma cell line **c** MCF7—Human breast carcinoma cell line **d** L_6—Rat myoblast cell line normal

SAR

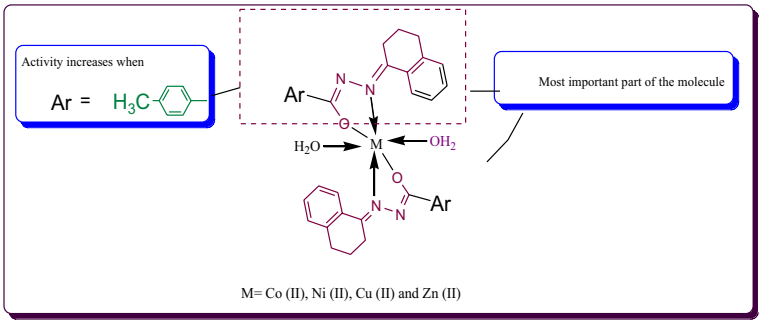

In conclusion, all the synthesized compounds (1–20) with different substituents were observed to be active against the three cancer cell lines (A549, Hela MCF7), but compound $[Cu(L^1)_2(H_2O)_2]$ (7) and $[Cu(L^3)_2(H_2O)_2]$ (15) was particularly more active. In methyl-substituted hydrazone moiety (HL^3) and when metal is copper, the electron releasing group in benzene ring increases the activity of the ring. However, HL^1 itself was not significantly active against the tested cell lines, but its

complexation with copper (7) resulted in a sudden rise in anticancer activity in case of A549, HeLa and MCF-7, cell lines with IC_{50} values of 13.28, 10.98 and 12.41 µg/mL, respectively, whereas towards normal cell line the compound was found to be non-toxic with an IC_{50} value of 16.42 µg/mL (Table 4). The activity also significantly increased for compounds 7 and 8 when metal was substituted with copper and zinc; the copper complex was more active than zinc. On the other hand, the complexation of HL^1 with nickel (compound 6) also showed moderate activity, but its complexation with cobalt (compound 5) did not produce more favourable effect.

The activity was found to be better when para-substituted pyridine ring (HL^4) was present as compared to meta-substituted pyridine ring (HL^1) in the hydrazones. Complexation of HL^4 with copper and zinc (compounds 19 and 20) further enhances the activity up to moderate level, but its complexation with cobalt and nickel (compounds 17 and 18) was not so effective.

Ligand HL^3 (methyl-substituted benzene) was highly active against MCF7 cell line as well as it was good active against A549 and HeLa cell lines, which showed its highest activity among all the four synthesized ligands, indicating that substitution with the methyl group on the benzene ring enhances anticancer activity. The complexation of HL^3 with copper and zinc leads to an even further increase in the activity. On the other hand, when M was replaced with nickel and copper (compounds 14 and 15) activity increases indicating the effectiveness of complexation.

Finally, we conclude that upon complexation in most cases there is enhancement in anticancer activity. Among all the synthesized compounds, complex $[Cu(L^3)_2(H_2O)_2]$ (15) displayed promising anticancer activity in case of A549, HeLa and MCF-7 cell lines with IC_{50} values of 12.81, 15.82 and 10.76 µg/mL, respectively, whereas towards normal cell line the compound was found to be non-toxic with an IC_{50} value of 16.30 µg/mL (Table 4), that was about eightfold less toxic than the standard drug doxorubicin (IC_{50} = 2.15 µg/mL). This high activity of compound 15 is due to electron-releasing methyl group in benzene ring, which increases the electron delocalization on benzene ring. Compounds 3, 7, 8, 9, 11, 12, 13, 14 and 16 also showed potential activity with $IC_{50} < 20$ µg/mL, while 2, 6, 10, 18, 19 and 20 showed moderate anticancer activity, and all other compounds were not found to have any significant activity. The hydrazones (1–4) and their complexes were observed to be low toxic against normal cell line.

Conclusion

Four new hydrazone ligands (1–4) and their corresponding metal complexes (5–20) were synthesized and properly characterized by spectroscopic techniques (FT-IR, NMR, UV–Vis, ESR, mass and fluorescence) and by physical analysis. The data revealed that hydrazones are bidentate (NO) in nature, and they bind to divalent metal ion with a nitrogen of (C=N) and carbonyl oxygen in enolized form giving stable octahedral complexes of type $[M(L^{1-4})_2(H_2O)_2]$. All the complexes are nonelectrolyte in nature and stable up to 180 °C, which suggests no hydrated water molecules outside the coordination sphere. Antimicrobial assessment of compounds shows that transition metal complexes (5–20) are more potent than their respective hydrazones and complexes 15 and 16 are more active. The results of cytotoxic potential of synthesized

compounds were good and copper complexes 7 and 15 were as most potent compound in the series against A549, HeLa and MCF-7 cancer cell lines, and their toxicity was eight times less than standard doxorubicin against normal line (L_6). The results obtained from the antimicrobial data suggest analogous relation with cytotoxicity results, which shows that the copper complex 15 was more biologically active in both studies, and all the compounds have low toxicity towards normal cell line(L_6) than the standard drug doxorubicin. Thus, based on the study in the present manuscript the complexes 7 and 15 may be regarded as good cytotoxic drug which encourage the candidates to synthesize various metallopharmaceuticals for further in vivo studies.

Supplementary information The online version of this article (https://doi.org/10.1007/s11164-021-04413-x)

Acknowledgements One of the authors Mr Som Sharma (JRF) is highly grateful to CSIR, New Delhi, India (No. 09/752(0060)/2016/EMR), for the grant of JRF scholarship and also thankful to Dr. A.P.J. Abdul Kalam Central Instrumentation Laboratory, and Department of Chemistry, GJUS&T, Hisar for supplying good facilities to perform this research work.

Compliance with ethical standards

Conflict of interest The authors declare no conflict of interest.

References

1. C. Elamathi, R. Butcher, R. Prabhakaran, Appl. Organomet. Chem. **32**, e4364 (2018)
2. A. Persidis, Nat. Biotechnol. **17**, 94 (1999)
3. I. Shagufta, Ahmad. Inorg. Chim. Acta. **506**, 119521 (2020)
4. H. Chakraborty, N. Paul, M.L. Rahman, Trans. Met. Chem. **19**, 524 (1994)
5. N.V. Kulkarni, N.H. Bevinahalli, V.K. Revankar, J. Coord. Chem. **63**, 1785 (2010)
6. T.A. Youssef, J. Coord. Chem. **61**, 816 (2008)
7. V.P. Singh, A. Katiyar, S. Singh, Biometals **21**, 491 (2008)
8. M.M.E. Shakdofa, F.A. El-Saied, A.J. Rasras, A.N. Al-Hakimi, Appl. Organomet. Chem. **32**, e4376 (2018)
9. F. Samy, M. Shebl, Appl. Organomet. Chem. **34**, e5502 (2020)
10. M. Shebl, A.A. Saleh, S.M.E. Khalil, M. Dawy, A.A.M. Ali, Inorg. Nano-Metal. Chem. **51**, 195 (2021)
11. M. Shebl, J. Mol. Struct. **79**, 1128 (2017)
12. G.S.S. Firmino, M.V.N. de Souza, C. Pessoa, M.C.S. Lourenco, J.A.L.C. Resende, J.A. Lessa, Biometals **29**, 953 (2016)
13. M. El-Behery, H. El-Twigry, Spectrochim. Acta. A. **66**, 28 (2007)
14. M. Shebl, S.M.E. Khalil, M.A.A. Kishk, D.M. El-Mekkawi, M. Saif, Appl. Organometal. Chem. **33**, 5147 (2019)
15. J. Wahbeh, S. Milkowski, Slas. Technol. Trans. Life. Sci. Innov. **24**, 161 (2019)
16. H. Hosseini-Monfared, A. Farrokhi, S. Alavi, P. Mayer, Trans. Met. Chem. **38**, 267 (2013)
17. S. Prasad, R.K. Agarwal, Res. Lett. Inorg. Chem. **2008**, 1 (2008)
18. M. Bakir, I. Hassan, T. Johnson, O. Brown, O. Green, C. Gyles, M.D. Coley, J. Mol. Struct. **688**, 213 (2004)
19. X. Ge, I. Wendler, P. Schramel, A. Kettrup, React. Funct. Polym. **61**, 1 (2004)
20. M. Taha, S.A.A. Shah, S. Imran, M. Afifi, S. Chigurupati, M. Selvaraj, F. Rahim, H. Ullah, K. Zaman, S. Vijayabalan, Bioorg. Chem. **75**, 78 (2017)
21. J. Devi, S. Kumari, S. Devi, R. Malhotra, P. Kumar, B. Narasimhan, Monatsh. Chem. **146**, 1995 (2015)

22. R.M. Beteck, L.J. Legoabe, M. Isaacs, S.D. Khanye, D. Laming, H.C. Hoppe, Medicina **55**, 206 (2019)
23. B.P. Bandgar, S.S. Gawande, R.G. Bodade, J.V. Totre, C.N. Khobragade, Bioorg. Med. Chem. **18**, 1364 (2010)
24. M. Mellado, A. Madrid, M. Reyna, C. Weinstein-Oppenheimer, J. Mella, C.O. Salas, E. Sánchez, M. Cuellar, Med. Chem. Res. **27**, 2414 (2018)
25. L.J. Legoabe, A. Petzer, J.P. Petzer, Bioor. Med. Chem. Lett. **24**, 2758 (2014)
26. J.R. Anacona, G. Calvo, J. Camus, Monatsh. Chem. **147**, 725 (2016)
27. J. Devi, N. Batra, R. Malhotra, Spectrochim. Acta. A. **97**, 397 (2012)
28. A.I. Vogel in the text book of quantitative chemical analysis, 5th edn. (Longmans, Edison, Wesley, London, 1999)
29. J. Devi, M. Yadav, A. Kumar, A. Kumar, Chem. Pap. **72**, 2479 (2018)
30. T. Mosmann, J. Immunol. Meth. **65**, 55 (1983)
31. W.J. Geary, Coord. Chem. Rev. **7**, 81 (1971)
32. I.B. Amali, M.P. Kesavan, V. Vijayakumar, N. Indra Gandhi, J. Rajesh, G. Rajagopal, J. Mol. Struct. **1183**, 342 (2019)
33. A.B. Garin, D. Rakarić, E.K. Andrić, M.M. Kosanović, T. Balić, F. Perdih, Polyhedron **166**, 226 (2019)
34. M. Shebl, S.M.E. Khalil, Monatsh. Chem. **146**, 15 (2015)
35. H.S. Seleem, B.A. El-Shetary, M. Shebl, Heteroatom. Chem. **18**, 100 (2007)
36. S.P. Perlepes, D. Nicholls, M.R. Harrison, Inorg. Chim. Acta. **102**, 137 (1985)
37. J. Devi, N. Batra, Spectrochim. Acta. A. **135**, 710 (2015)
38. S.N. Choi, E.R. Menzel, J.R. Wasson, J. Inorg. Nucl. Chem. **39**, 417 (1977)
39. T.R. Reddy, R. Srinivasan, J. Chem. Phys. **43**, 1404 (1965)
40. M.A. Diab, A.Z. El-Sonbati, A.A. El-Bindary, G.G. Mohamed, Sh.M. Morgan, Res. Chem. Intermed. **41**, 9029 (2015)
41. J. Devi, M. Yadav, D.K. Jindal, D. Kumar, Y. Poornachandra, Appl. Organomet. Chem. **33**, e5154 (2019)
42. S. Chandra, L.K. Gupta, Spectrochim. Acta. A. **62**, 307 (2005)
43. M. Shebl, O.M.I. Adly, A. Taha, N.N. Elabd, J. Mol. Struct. **438**, 1147 (2017)
44. A.D. Kulkarni, S.A. Patil, P.S. Badami, J. Sulf. Chem. **30**, 145 (2009)
45. A.K. Singh, R. Singh, P. Saxena, Trans. Met. Chem. **29**, 867 (2004)
46. K. Jayanthi, K. Fazl-Ur-Rahman, P.V. Kamath, G. Periyasamy, Spectrochim. Acta. A. **233**, 118192 (2020)
47. N. Zhang, Y.H. Fan, C.F. Bi, X. Zhang, P.F. Zhang, Z.Y. Zhang, X. Li, J. Inorg. Organomet. Polym. **23**, 1492 (2013)
48. A. Majumder, G.M. Rosair, A. Mallick, N. Chattopadhyay, S. Mitra, Polyhedron **25**, 1753 (2006)
49. H.F. El-Shafiy, M. Shebl, J. Mol. Struct. **403**, 1156 (2018)
50. M. Shebl, M. Saif, A.I. Nabeel, R. Shokry, J. Mol. Struct. **335**, 1118 (2016)
51. M. Shebl, Spectrochim. Acta A **117**, 127 (2014)
52. S.A. Aly, S.K. Fathalla, Arab. J. Chem. **13**, 3735 (2020)
53. M. Shebl, J. Coord. Chem. **69**, 199 (2016)
54. J. Devi, M. Yadav, D. Kumar, L.S. Naik, D.K. Jindal, Appl. Organomet. Chem. **33**, e4693 (2019)
55. J. Devi, J. Yadav, D. Kumar, D.K. Jindal, B. Basu, Appl. Organomet. Chem. **34**, e5815 (2020)
56. N. Raman, A. Selvan, J. Coord. Chem. **64**, 534 (2011)
57. A. Mai-Prochnow, M. Clauson, J. Hong, A.B. Murphy, Sci. Rep. **6**, 38610 (2016)
58. Z. Breijyeh, B. Jubeh, R. Karaman, Molecules **25**, 1340 (2020)
59. K. Tummalapalli, V.C.S.P. Munusami, M. Pathak, M.M. Be, Appl. Organomet. Chem. **31**, 3680 (2017)
60. M.V. Angelusiu, S.F. Barbuceanu, C. Draghici, G.L. Almajan, Euro. J. Med. Chem. **45**, 2056 (2010)
61. J. Devi, J. Yadav, N. Singh, Res. Chem. Intermed. **45**, 3943 (2019)
62. A. Chaudhary, R.V. Singh, Phosphorus. Sulfur. Silicon. Relat. Elem. **178**, 603 (2003)
63. E. Narvi, K. Jaakkola, S. Winsel, C. Oetken-Lindholm, P. Halonen, L. Kallio, M.J. Kallio, Br. J. Cancer. **108**, 82 (2013)
64. J.D. Chellaian, J. Johnson, Spectrochim. Acta. A. **127**, 396 (2014)